for the disruption of the barrier function of TJs by C-CPE and for its interaction with claudin-4 [12], and we show here that aromatic and hydrophobic properties of Tyr at position 306 is partly important for the C-CPE activities.

Because CPE is a foodborne toxin in humans, its functional domains have been mapped in many studies. C-CPE is the C-terminal fragment of CPE and is responsible for binding of CPE to its receptor [19]. Hanna et al. showed that the C-terminal 30 amino acids of CPE mediates binding to its receptor, claudin-4 [20]. We previously show that deletion of the C-terminal 16 amino acids of C-CPE eliminates the TJ-modulating activity of C-CPE [11] and that the tyrosine residues (Tyr306, 310, 312) in the 16 amino acids of C-CPE are responsible for the C-CPE activity [12]. Substitution of Tyr306 with Ala reveals that Tyr306 is a pivotal residue for the abilities of C-CPE to bind claudin-4 and modulate the TJ barrier [12].

What means the attenuation of the C-CPE activities by mutation of Tyr306 to Ala in C-CPE? Tyr is a polar, hydrophobic and aromatic residue, but Ala is a non-polar, non-hydrophobic and non-aromatic residue. Therefore, we suspected that polar, hydrophobic and/or the aromatic property of Tyr is important for the activities of C-CPE. We prepared Y306F (aromatic and hydrophobic mutant), Y306W (aromatic, hydrophobic and polar mutant), and Y306K (polar and positive charged mutant) mutants and examined their abilities to modulate the TJ barrier function and bind claudin-4. Replacement of Tyr with Phe did not affect these activities, whereas replacement with Lys attenuated these activities, and mutation to Trp caused a partial reduction in both activities. These findings suggest that the aromatic and hydrophobic properties of Tyr at position 306 are important for the activities of C-CPE and hydrogen bonding potential of Tyr at position 306 is not essential for them.

How does Tyr306 contribute to modulation of the TJ barrier function and to the interaction with claudin-4? Considering the mode of action of C-CPE as a claudin modulator, this leaves the question of whether it is possible to separate the ability of C-CPE to modulate the TJ barrier function and its ability to interact with claudin. Deletion of the C-terminal region of C-CPE and substitution of Tyr306 with Ala in C-CPE eliminate these activities [10–12]. Similarly, we showed here that mutation of Tyr306 to Lys reduces both the ability to modulate the TJ barrier function and the ability to bind claudin-4. These findings suggest that the abilities of C-CPE to bind to claudin-4 and modulate TJ-barrier cannot be separated in Tyr306 mutants. Tsukita lab found that CPE interacted with claudin via extracellular loop domain of claudin and claudin was degraded by endocytotic pathway in C-CPE-treated cells [9,21]. We also found that loss of interaction of C-CPE with claudin-4 by deletion of the C-terminal C-CPE [10,11]. These findings indicate that interaction of C-CPE with claudin is the first step in the modulation of TJ-barrier by C-CPE. Tyr306 may be partly critical for interaction of C-CPE with claudin. Since Y306F mutant binds to claudin-4, interaction of C-CPE with claudin-4 may not be mediated by hydrogen bond. Mutation of Tyr to Trp at position 306 resulted in C-CPE with subtle differences in claudin-4 binding. In contrast, Y306K and Y306A mutants reduced binding to claudin-4. Taken together, the hydrophobicity at position 306 may be important for binding of C-CPE to claudin-4. An aromatic/polar amino acid at position 306 might be critical for the correct folding of C-CPE, which might expose other residues and allow them to reach their target site on claudin-4.

Determination of the three-dimensional structures of CPE and claudin is critical for elucidation of the precise mechanism of interaction between C-CPE and claudin-4, but, because these proteins are hydrophobic, this has not yet been accomplished. In the meantime, our findings should help to clarify how these two proteins interact and to prepare a novel claudin-modulator using C-CPE as a prototype.

Acknowledgements

We thank Dr. Y. Tsutsumi and all members of our laboratory for their helpful comments and discussion. We also thank Drs. S. Tsukita and M. Furuse for providing claudin-4-expressing cells. This study was partly supported by a Grand-in-Aid from the Ministry of Education, Science, and Culture of Japan, a SHISEIDO Grant for Scientific Research, Takeda Science Foundation, Mochida Memorial Foundation for Medical and Pharmaceutical Research, and the Cosmetology Research Foundation.

REFERENCES

[1] Powell DW. Barrier function of epithelia. Am J Physiol 1981;241:G275–88.
[2] Tsukita S, Furuse M. Pores in the wall: claudins constitute tight junction strands containing aqueous pores. J Cell Biol 2000;149:13–6.
[3] Furuse M, Hata M, Furuse K, Yoshida Y, Haratake A, Sugitani Y, et al. Claudin-based tight junctions are crucial for the mammalian epidermal barrier: a lesson from claudin-1-deficient mice. J Cell Biol 2002;156:1099–111.
[4] Nitta T, Hata M, Gotoh S, Seo Y, Sasaki H, Hashimoto N, et al. Size-selective loosening of the blood–brain barrier in claudin-5-deficient mice. J Cell Biol 2003;161:653–60.
[5] Furuse M, Sasaki H, Tsukita S. Manner of interaction of heterogeneous claudin species within and between tight junction strands. J Cell Biol 1999;147:891–903.
[6] Furuse M, Furuse K, Sasaki H, Tsukita S. Conversion of zonulae occludentes from tight to leaky strand type by introducing claudin-2 into madin-darby canine kidney I cells. J Cell Biol 2001;153:263–72.
[7] McClane BA, Chakrabarti G. New insights into the cytotoxic mechanisms of *Clostridium perfringens* enterotoxin. Anaerobe 2004;10:107–14.
[8] Katahira J, Inoue N, Horiguchi Y, Matsuda M, Sugimoto N. Molecular cloning and functional characterization of the receptor for *Clostridium perfringens* enterotoxin. J Cell Biol 1997;136:1239–47.
[9] Sonoda N, Furuse M, Sasaki H, Yonemura S, Katahira J, Horiguchi Y, et al. *Clostridium perfringens* enterotoxin fragment removes specific claudins from tight junction strands: evidence for direct involvement of claudins in tight junction barrier. J Cell Biol 1999;147:195–204.
[10] Kondoh M, Masuyama A, Takahashi A, Asano N, Mizuguchi H, Koizumi N, et al. A novel strategy for the enhancement of drug absorption using a claudin modulator. Mol Pharmacol 2005;67:749–56.
[11] Takahashi A, Kondoh M, Masuyama A, Fujii M, Mizuguchi H, Horiguchi Y, et al. Role of C-terminal regions of the C-terminal fragment of *Clostridium perfringens* enterotoxin in

its interaction with claudin-4. J Control Release 2005;108:56–62.
[12] Harada M, Kondoh M, Ebihara C, Takahashi A, Komiya E, Fujii M, et al. Role of tyrosine residues in modulation of claudin-4 by the C-terminal fragment of *Clostridium perfringens* enterotoxin. Biochem Pharmacol, in press.
[13] Morita K, Furuse M, Fujimoto K, Tsukita S. Claudin multigene family encoding four-transmembrane domain protein components of tight junction strands. Proc Natl Acad Sci USA 1999;96:511–6.
[14] Ebihara C, Kondoh M, Hasuike N, Harada M, Mizuguchi H, Horiguchi Y, et al. Preparation of a Claudin-targeting molecule using a C-terminal fragment of *Clostridium perfringens* enterotoxin. J Pharmacol Exp Ther 2006;316:255–60.
[15] Leamon CP, Pastan I, Low PS. Cytotoxicity of folate-*Pseudomonas* exotoxin conjugates toward tumor cells. J Biol Chem 1993;268:24847–54.
[16] Mesri EA, Ono M, Kreitman RJ, Klagsbrun M, Pastan I. The heparin-binding domain of heparin-binding EGF-like growth factor can target *Pseudomonas* exotoxin to kill cells exclusively through heparan sulfate proteoglycans. J Cell Sci 1994;107:2599–608.
[17] Beers R, Chowdhury P, Bigner D, Pastan I. Immunotoxins with increased activity against epidermal growth factor receptor vIII-expressing cells produced by antibody phage display. Clin Cancer Res 2000;6:2835–43.
[18] Sallee VL, Wilson FA, Dietschy JM. Determination of undirectional uptake rates for lipids across the intestinal brush border. J Lipid Res 1972;12:184–92.
[19] Horiguchi Y, Akai T, Sakaguchi G. Isolation and function of a *Clostridium perfringens* enterotoxin fragment. Infect Immun 1987;55:2912–5.
[20] Hanna PC, Mietzner TA, Schoolnik GK, McClane BA. Localization of the receptor-binding region of *Clostridium perfringens* enterotoxin utilizing cloned toxin fragments and synthetic peptides. J Biol Chem 1991;266: 11037–43.
[21] Fujita K, Katahira J, Horiguchi Y, Sonoda N, Furuse M, Tsukia S. *Clostridium perfringens* enterotoxin binds to the second extracellular loop of claudin-3, a tight junction integral membrane protein. FEBS Lett 2000;476:258–61.

Fiber-Modified Adenovirus Vectors Decrease Liver Toxicity through Reduced IL-6 Production[1]

Naoya Koizumi,*† Tomoko Yamaguchi,* Kenji Kawabata,* Fuminori Sakurai,* Tomomi Sasaki,* Yoshiteru Watanabe,† Takao Hayakawa,‡ and Hiroyuki Mizuguchi[2]*§

Adenovirus (Ad) vectors are one of the most commonly used viral vectors in gene therapy clinical trials. However, they elicit a robust innate immune response and inflammatory responses. Improvement of the therapeutic index of Ad vector gene therapy requires elucidation of the mechanism of Ad vector-induced inflammation and cytokine/chemokine production as well as development of the safer vector. In the present study, we found that the fiber-modified Ad vector containing poly-lysine peptides in the fiber knob showed much lower serum IL-6 and aspartate aminotransferase levels (as a maker of liver toxicity) than the conventional Ad vector after i.v. administration, although the modified Ad vector showed higher transgene production in the liver than the conventional Ad vector. RT-PCR analysis showed that spleen, not liver, is the major site of cytokine, chemokine, and IFN expression. Splenic CD11c$^+$ cells were found to secret cytokines. The tissue distribution of Ad vector DNA showed that spleen distribution was much reduced in this modified Ad vector, reflecting reduced IL-6 levels in serum. Liver toxicity by the conventional Ad vector was reduced by anti-IL-6R Ab, suggesting that IL-6 signaling is involved in liver toxicity and that decreased liver toxicity of the modified Ad vector was due in part to the reduced IL-6 production. This study contributes to an understanding of the biological mechanism in innate immune host responses and liver toxicity toward systemically administered Ad vectors and will help in designing safer gene therapy methods that can reduce robust innate immunity and inflammatory responses. ***The Journal of Immunology,*** **2007, 178: 1767–1773.**

Recombinant adenovirus (Ad)[3] vectors are widely used for gene therapy experiments and clinical gene therapy trials. One of the limitations of Ad vector-mediated gene transfer is the immune response after systemic administration of the Ad vector (1, 2). The immune response to the Ad vector and Ad vector-transduced cells dramatically affects the kinetics of the Ad vector-delivered genes and the gene products. The potent immunogenic toxicities and consequent short-lived transgene expression of Ad vectors are undesirable properties if Ad vectors are to be more broadly applied. The immunogenic toxicities associated with the use of Ad vectors involve both innate and adaptive immune responses.

In the first generation Ad vector lacking the *E1* gene, leaky expression of viral genes from the vector stimulates an immune response against the Ad vector-transduced cells (3–5). The CTL response can be elicited against viral gene products and/or transgene products expressed by transduced cells. The molecular mechanism of this toxicity has been studied extensively, and the helper-dependent (gutted) Ad vector, which deletes all of the viral protein-coding sequences, has been developed to overcome this limitation (6–8). The humoral virus-neutralizing Ab responses against the Ad capsid itself are another limitation, preventing transgene expression upon the subsequent administration of vectors of the same serotype. Because hexons are mainly targeted by neutralizing Abs, hexon modification has been reported to allow for escape from neutralizing Abs (9). The Ad vectors belonging to types of the subgroup other than Ad type 5, including an Ad type 11- or 35-based vector, or to species other than human have also been developed (10–13).

Regarding the innate immune response, shortly after systemic injection of the Ad vector cytokines/chemokines are produced and an inflammatory response occurs in response to the Ad vector and Ad vector-transduced cells. It has been reported that activated Kupffer cells (and monocytes and resident macrophages) and dendritic cells (DC) release proinflammatory cytokines/chemokines such as IL-6, TNF-α, IP-10, and RANTES, causing the activation of an innate immune response (14, 15). NF-κB activation is likely to play a central role in inflammatory cytokine/chemokine production (16, 17). Although many papers regarding the innate immune response to the Ad vector have been published thus far, the biological mechanism has not been clearly elucidated. Even the cell types responsible for the innate immune response have not been identified. Understanding the mechanism of and identifying the cell types responsible for the innate immune response and liver inflammation are crucial to the construction of new vectors that are safer and efficiently transduce target tissue. Modification of the Ad vector with polyethylene glycol (PEG) reduces the innate immune response and also prolongs persistence in the blood and circumvents neutralization of the Ad vectors by Abs (18–21). We have previously reported that the mutant Ad vector ablating coxsackievirus and Ad receptor (CAR) (the first receptor) binding, α_v integrin (the secondary receptor) binding, and heparan sulfate glycosaminoglycan (HSG) (the third receptor) binding reduced (or blunted)

*Laboratory of Gene Transfer and Regulation, National Institute of Biomedical Innovation, Osaka, Japan; †Department of Pharmaceutics and Biopharmaceutics, Showa Pharmaceutical University, Tokyo, Japan; ‡Pharmaceuticals and Medical Devices Agency, Tokyo, Japan; and §Graduate School of Pharmaceutical Sciences, Osaka University, Osaka, Japan

Received for publication August 29, 2006. Accepted for publication November 10, 2006.

The costs of publication of this article were defrayed in part by the payment of page charges. This article must therefore be hereby marked *advertisement* in accordance with 18 U.S.C. Section 1734 solely to indicate this fact.

[1] This work was supported by grants from the Ministry of Health, Labor, and Welfare of Japan.

[2] Address correspondence and reprint requests to Dr. Hiroyuki Mizuguchi, Laboratory of Gene Transfer and Regulation, National Institute of Biomedical Innovation, Asagi 7-6-8, Saito, Ibaraki, Osaka 567-0085, Japan. E-mail address: mizuguch@nibio.go.jp

[3] Abbreviations used in this paper: Ad, adenovirus; AST, aspartate aminotransferase; CAR, coxsackievirus and Ad receptor; DC, dendritic cell; HSG, heparan sulfate glycosaminoglycan; PEG, polyethylene glycol; VP, virus particle.

liver toxicity and IL-6 production (22). However, these two Ad vectors mediate significantly lower tissue transduction due to steric hindrance by PEG chains and a loss of binding activity to the receptor, respectively (20–22). An Ad vector showing efficient transduction and reduced innate immune response has not yet been developed.

In the present study, we elucidate the molecular mechanism of the innate immune response by the Ad vector and characterize the safer Ad vector, which reduces the innate immune response and liver toxicity. We found that the fiber-modified Ad vector containing a stretch of lysine residues (K7 (KKKKKKK) peptide) (23–25) that target heparan sulfates on the cellular surface greatly reduced IL-6 and liver toxicity after i.v. injection into mice compared with the conventional Ad vector. IL-6 and the other immune cytokines, chemokines, and IFNs were mainly produced from the spleen and especially from conventional DC ($CD11c^+B220^-$ cells), not the liver. The spleen distribution of the K7-modified Ad vector was reduced compared with the conventional Ad vector. The K7-modified Ad vector decreased the liver toxicity (aspartate aminotransferase (AST) levels), at least in part due to the reduced serum IL-6 levels. Importantly, this K7-modified Ad vector maintained high transduction efficiency in vivo and showed somewhat higher transgene production in the liver than a conventional Ad vector.

Materials and Methods

Ad vector

Two luciferase-expressing Ad vectors, Ad-L2 and AdK7-L2, have been constructed previously (25, 26). The CMV promoter-driven luciferase gene derived from the pGL3-Control was inserted into the E1 deletion region of the Ad genome. Ad-L2 contains wild-type fiber, whereas AdK7-L2 contains the polylysine peptide KKKKKKK in the C-terminal of the fiber knob (25). Viruses (Ad-L2 and AdK7-L2) were prepared as described previously (25) and purified by $CsCl_2$ step gradient ultracentrifugation. Determination of virus particle titers was accomplished spectrophotometrically by the method of Maizel et al. (27).

Ad-mediated transduction in vivo

Ad-L2 or AdK7-L2 were i.v. administered to C57BL6 mice (1.0×10^{10} virus particles (VP)) (6-wk-old males obtained from Nippon SLC). Forty-eight hours later, the heart, lung, liver, kidney, and spleen were isolated and homogenated as previously described (28). Luciferase production was determined using a luciferase assay system (PicaGene 5500; Toyo Inki). Protein content was measured with a Bio-Rad assay kit using BSA as a standard.

The amounts of Ad genomic DNA in the each organ were quantified with the TaqMan fluorogenic detection system (ABI Prism 7700 sequence detector; PerkinElmer Applied Biosystems). Samples were prepared with DNA templates isolated from each organ (25 ng) by an automatic nucleic acid isolation system (NA-2000; Kurabo Industries). The amounts of Ad DNA were quantified with the TaqMan fluorogenic detection system (PerkinElmer Applied Biosystems) as described in our previous report (22).

To analyze the involvement of IL-6 signaling in liver toxicity in response to Ad vector administration, 100 μg per mouse of an anti-IL-6R Ab (clone D7715A7; BioLegend) that specifically blocks IL-6 signaling was i.p. administered to C57BL6 mice 1.5 h before Ad-L2 administration (3.0×10^{10} VP). Rabbit IgG (clone R3-34; BD Biosciences) was administered as a control. Serum samples and liver tissue were collected 48 h later, and AST levels in the serum and luciferase production in the liver were determined.

Liver serum enzymes and cytokine levels after systemic administration

Blood samples were collected by the inferior vena cave at the indicated times (3 or 48 h) after i.v. administration of Ad-L2 or AdK7-L2 (3.0×10^{10} and 1.0×10^{11} VP, respectively). IL-6 and IL-12 levels in serum samples collected at 3 h after Ad injection were measured by an ELISA kit (BioSource International). The levels of AST in serum samples collected at 24 and 48 h were measured with the Transaminase-CII kit (Wako Pure Chemical). Forty-eight hours after the Ad vector injection, the mice were killed and their livers were collected. The liver was washed, fixed in 10% formalin, and embedded in paraffin. After sectioning, the tissue was dewaxed in ethanol, rehydrated, and stained with H&E. This process was commissioned to the Applied Medical Research Laboratory (Osaka, Japan).

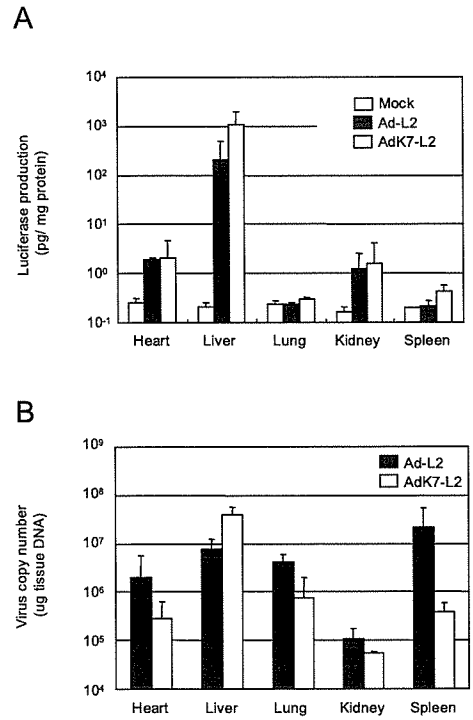

FIGURE 1. Luciferase production and biodistribution of viral DNA after the i.v. administration of Ad-L2 or AdK7-L2 into mice. Ad-L2 or AdK7-L2 (1.0×10^{10} VP) was i.v. injected into the mice. Forty-eight hours later, the heart, lung, liver, kidney, and spleen were harvested, and luciferase production (*A*) and Ad vector DNA (*B*) in each organ were measured by a luciferase assay system or the quantitative TaqMan PCR assay, respectively. All data represent the means ± SD of 4–6 mice.

Cytokines and chemokines mRNA levels in tissue after systemic administration

Total tissue RNA samples were isolated by the reagent ISOGEN (Wako Pure Chemical) 3 h after the i.v. administration of Ad-L2 or AdK7-L2 (1.0×10^{11} VP). Reverse transcription was performed using the SuperScript first-strand synthesis system for first-strand cDNA synthesis (Invitrogen Life Technologies) according to the instructions of the manufacturer. IL-6 and IL-12 mRNA in the liver and spleen were quantified with the TaqMan fluorogenic detection system (PerkinElmer Applied Biosystems). Semiquantified RT-PCR analysis was also performed to determine mRNA levels of the cytokines, chemokines, and IFNs (total eight mRNA). The primer sequences and probes were as follows: IL-6 forward, 5′-GAG GAT ACC ACT CCC AAC AGA CC-3′; IL-6 reverse, 5′-AAG TGC ATC ATC GTT GTT CAT ACA-3′ (reverse); IL-6 probe, 5′-CAG AAT TGC CAT TGC ACA ACT CTT TTC TCA-3′; IL-12p40 forward, 5′-GGA AGC ACG GCA GCA GAA TA-3′; IL-12p40 reverse, 5′-AAC TTG AGG GAG AAG TAG GAA TGG-3′; IL-12p40 probe, 5′-CAT CAT CAA ACC AGA CCC GCC CAA-3′; TNF-α forward, 5′-CCT GTA GCC CAC GTC GTA GC-3′; TNF-α reverse, 5′-TTG ACC TCA GCG CTG AGT TG-3′; RANTES forward, 5′-ATG AAG ATC TCT GCA GCT GCC CTC ACC-3′; RANTES reverse, 5′-CTA GCT CAT CTC CAA ATA GTT GAT G-3′; MIP-2 forward, 5′-ACC TGC CGG CTC CTC AGT GCT GC-3′; MIP-2 reverse, 5′-GGC TTC AGG GTC AAG GCA AAC-3′; IFN-α forward, 5′-AGG CTC AAG CCA TCC CTG T-3′; IFN-α reverse, 5′-AGG CAC AGG GGC TGT CTT TCT TCT-3′; IFN-β forward, 5′-TTC CTG CTG TGC TTC TCC AC-3′; IFN-β reverse, 5′-GAT TCA CTA CCA GTC CCA GAG TC-3′; IFN-γ forward, 5′-GAG GAT ACC ACT CCC AAC AGA CC-3′; IFN-γ reverse, 5′-AAG TGC ATC ATC GTT GTT CAT ACA-3′; GAPDH forward, 5′-TTC ACC ACC ATG GAG AAG GC-3′; and GAPDH reverse, 5′-GGC ATG GAC TGT GGT CAT GA-3′. The expected sizes of the PCR products are as follows: IL-6, 193 bp; IL-12p40, 155 bp; TNF-α, 374 bp; RANTES, 252 bp; MIP-2, 221 bp; IFNα, 272 bp; IFNβ, 607 bp; IFN-γ, 306 bp; and GAPDH, 237 bp.

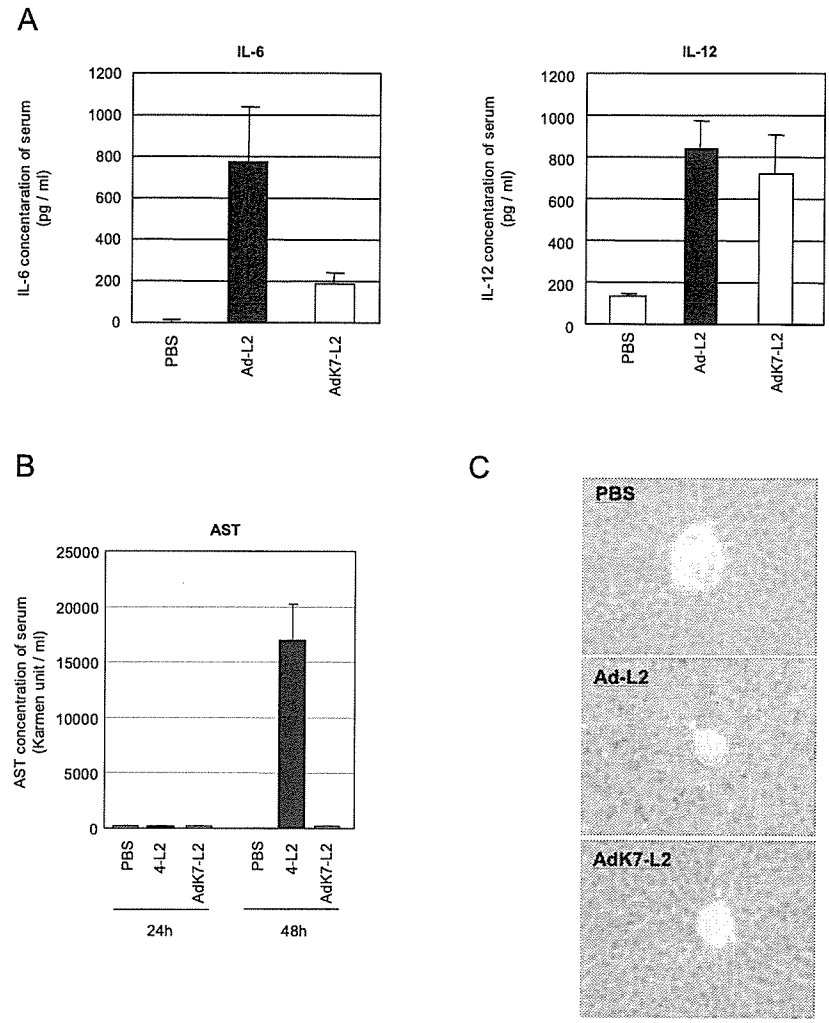

FIGURE 2. Cytokines and liver enzyme levels in serum after the systemic administration of Ad-L2 or AdK7-L2 into mice. Blood samples were collected by inferior vena cave at 3 h (*A*) or 24 and 48 h (*B*) after i.v. administration of Ad-L2 or AdK7-L2 (1.0×10^{11} VP for *A* or 3.0×10^{10} VP for *B*). The livers were collected after 48 h following the injection (3.0×10^{10} VP) (*C*). *A*, IL-6 and IL-12 levels in the serum were measured by ELISA. *B*, AST levels in the serum were measured using a Transaminase-CII kit. *C*, Paraffin sections of the livers were prepared. Each section was stained with H&E. Data represent the means ± SD of four mice.

Cell sorting of splenic cells

Splenic conventional DC, plasmacytoid DC, and B cells, which were $CD11c^+B220^-$, $CD11c^+B220^+$, and $CD11c^-B220^+$ cells, respectively, were sorted by FACS Aria (BD Biosciences). Total RNA samples were isolated from each cell by the reagent ISOGEN, and RT-PCR analysis was then performed as described above.

Results

This study was undertaken to elucidate the biological mechanism in the innate immune host responses toward i.v. administered Ad vector. The relationship between the innate immune response and liver toxicity by systemic administration of the Ad vectors was also examined.

Gene transduction and Ad vector accumulation in vivo

In this study we used the conventional Ad vector (Ad-L2) and a fiber-modified Ad vector containing a polylysine (K7) peptide (AdK7-L2), both of which express luciferase under the control of the CMV promoter. First, we examined luciferase production in the organ and the biodistribution of viral DNA after i.v. administration of AdK7-L2 (1.0×10^{10} VP) into mice compared with Ad-L2 (see Fig. 3). The vector dose of 1.0×10^{10} VP was selected because this dose did not induce any apparent toxicity (IL-6 and AST production) with either Ad-L2 or AdK7-L2. When a higher dose (3.0×10^{10} or 1.0×10^{11} VP) was used, only Ad-L2 and not AdK7-L2 showed toxicity (described later), which does not reflect an exact comparison of the transduction efficiency. The Ad type 5-based vector delivers the foreign gene predominantly in the liver after i.v. injection into mice (29, 30). Interestingly, AdK7-L2 mediated ~6-fold higher liver transduction than Ad-L2 (Fig. 1*A*). In contrast, the luciferase production in the heart, lung, kidney, and spleen in response to AdK7-L2 was similar to that in response to Ad-L2. To examine the biodistribution of Ad-L2 and AdK7-L2 in mice, the amounts of Ad DNA in each organ 48 h after the injection of Ad vectors were measured with the TaqMan fluorogenic detection system. More AdK7-L2 DNA accumulated in the liver than Ad-L2 DNA (Fig. 1*B*), although the amounts of AdK7-L2 DNA in the heart, lung, kidney, and spleen were less than those of Ad-L2 DNA. In particular, the amounts of AdK7-L2 DNA in the spleen were ~56-fold less than those of Ad-L2 DNA. The data regarding luciferase production (Fig. 1*A*) and the amounts of Ad DNA in most organs (Fig. 1*B*) showed discrepancies. Luciferase production in the liver was >2 log order higher than that in other organs, while the amounts of Ad DNA in liver were not as striking among the organs compared with luciferase production. This difference is likely due to the difference in the amount of nonspecific viral uptake among the organs. Reduced spleen accumulation of AdK7-L2 DNA, compared with Ad-L2 DNA, was also observed at a dose of 1.0×10^{11} VP (data not shown).

Serum cytokines and AST levels

The systemic administration of Ad vectors results in the initiation of strong innate immune responses and inflammation in animals and humans (1), and this toxicity limits the utility of Ad vectors for gene therapy. To evaluate the innate immune response and liver toxicity of each Ad vector, we measured the levels of IL-6, IL-12, and AST in serum. Because IL-6 in the serum and hepatic toxicity

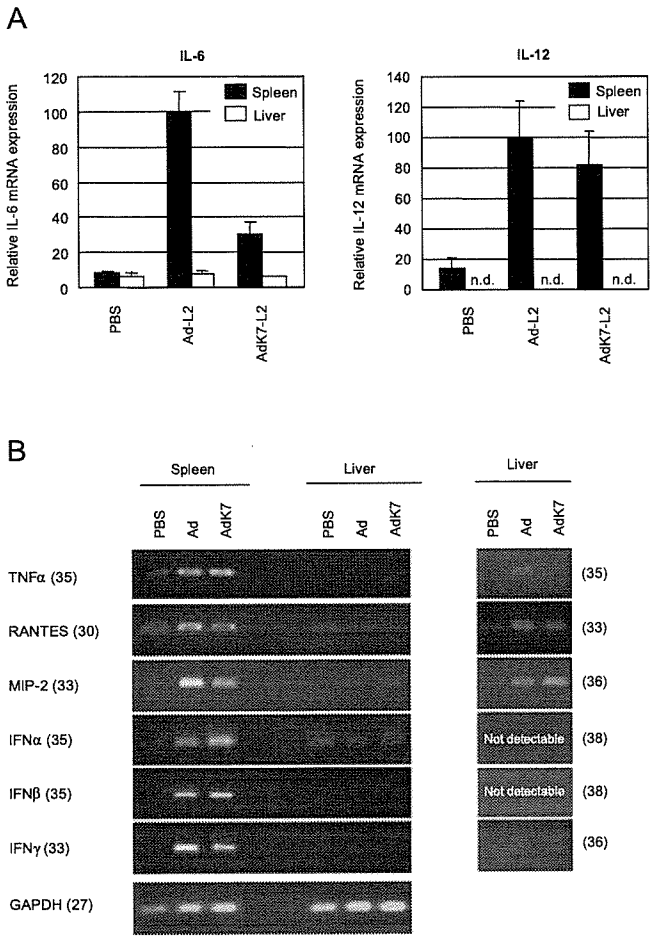

FIGURE 3. Cytokine, chemokine, and IFN mRNA levels in liver and spleen after the systemic administration of Ad-L2 or AdK7-L2 into mice. Total mRNA samples were isolated from liver and spleen at 3 h after i.v. administration of Ad-L2 or AdK7-L2 (1.0×10^{11} VP). After the reverse transcriptase reaction, IL-6 and IL-12 cDNA were measured with the quantitative TaqMan PCR assay (*A*). The expression of TNF-α, RANTES, MIP-2, IFN-α, IFN-β, and IFN-γ was measured by semiquantitative RT-PCR assay (*B*). All data represent the means ± SD of four mice. Cycle number is given in parentheses.

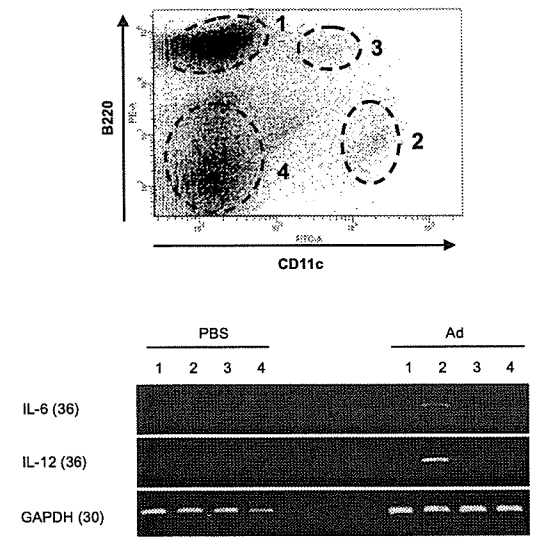

FIGURE 4. IL-6 and IL-12 mRNA levels in splenic CD11c-positive cells after the systemic administration of Ad-L2 into mice. Total mRNA samples were isolated from sorted splenic cells 3 h after i.v. administration of Ad-L2 (1.0×10^{11} VP). The expression levels of IL-6 and IL-12 mRNA were measured by RT-PCR assay. *Lane 1*, B cell ($B220^+CD11c^-$); *lane 2*, conventional DC ($B220^-CD11c^+$); *lane 3*, plasmacytoid DC ($B220^+CD11c^+$); *lane 4*, other cells ($B220^-CD11c^-$). Cycle number is given in parentheses.

analysis was detected at a dose of $>1.0 \times 10^{11}$ or 3.0×10^{10} VP, respectively, these doses were used.

IL-6 levels in response to AdK7-L2 were one-fourth of those with Ad-L2 (Fig. 2*A*). In contrast, there was no difference in serum IL-12 levels between Ad-L2 and AdK7-L2. Thus, IL-6 and IL-12 appear to be produced by a different mechanism. TNF-α in the serum after the injection of Ad-L2 or AdK7-L2 could not be detected (data not shown). Ad-L2 led to high levels of serum AST at 48 h after injection, while AdK7-L2 did not induce AST (Fig. 2*B*). At 24 h, neither Ad-L2 nor AdK7-L2 induced AST. In histological analysis, degranulation or denucleation occurred in hepatocytes from Ad-L2, while AdK7-L2 did not induce hepatocyte toxicity (Fig. 2*C*). The results using AdK7-L2 were similar to those in the untreated mice (Fig. 2, *B* and *C*), suggesting that AdK7-L2 does not show any liver toxicity. These results suggest that AdK7-L2 shows less IL-6 production and almost no liver toxicity.

Cytokines mRNA levels in liver and spleen cells

Ad vectors induce the expression of various cytokines and chemokines in the innate immune responses by effector cells such as macrophages and DC (15, 17, 31–33). Liver and spleen are two major organs responsible for the location of immune cells. We attempted to determine which organ (liver or spleen) produces cytokines, chemokines, and IFNs (IL-6, IL-12, TNF-α, RANTES, MIP-2, IFNα, IFNβ, and IFN-γ) by quantitative real-time RT-PCR or semiquantitative RT-PCR analysis. IL-6 and IL-12 mRNA levels were not induced in the liver after i.v. administration of Ad vectors (Fig. 3*A*). This result was also checked by the result that specific IL-6 and IL-12 mRNA bands were not detected in the liver by RT-PCR analysis (data not shown). Expression of TNF-α, RANTES, MIP-2, IFN-α, IFN-β, and IFN-γ mRNA was also detected mainly in the spleen, not the liver (Fig. 3*B*). IL-6, MIP-2, and IFN-γ mRNA levels in the spleen in response to AdK7-L2 were lower than those in response to Ad-L2. In the liver, TNF-α, RANTES, MIP-2, and IFN-γ mRNA were detected by a high cycle number of PCR after Ad (Ad-L2 or AdK7-L2) injection, whereas IFN-α and IFN-β could be not detected (Fig. 3*B*).

We next identified the cell types responsible for the IL-6 and IL-12 expression in the spleen after i.v. administration of the Ad vector (Ad-L2). Spleen cells were sorted by FACS Aria based on the expression of CD11c and B220 in conventional DC ($CD11c^+B220^-$), plasmacytoid DC ($CD11c^+B220^+$), and B cells ($CD11c^-B220^+$ cells). IL-6 and IL-12 mRNA were mainly detected in the splenic conventional DC. Only a faint band of IL-12 mRNA was also detected in the splenic plasmacytoid DC ($CD11c^+B220^+$) (Fig. 4). These results suggest that splenic conventional DC are major effector cells of innate immune response (at least IL-6 and IL-12 production) against systemically administered Ad vectors.

Elimination of IL-6 signaling reduces liver toxicity

It has previously been shown that TNF-α is likely to be involved in host responses to Ad vectors in vitro and in vivo (34). Recently, Shayakhmetov et al. (35) have reported that IL-1 signaling, not TNF-α signaling, is involved in Ad vector-associated liver toxicity after i.v. administration. However, the mechanism of liver toxicity

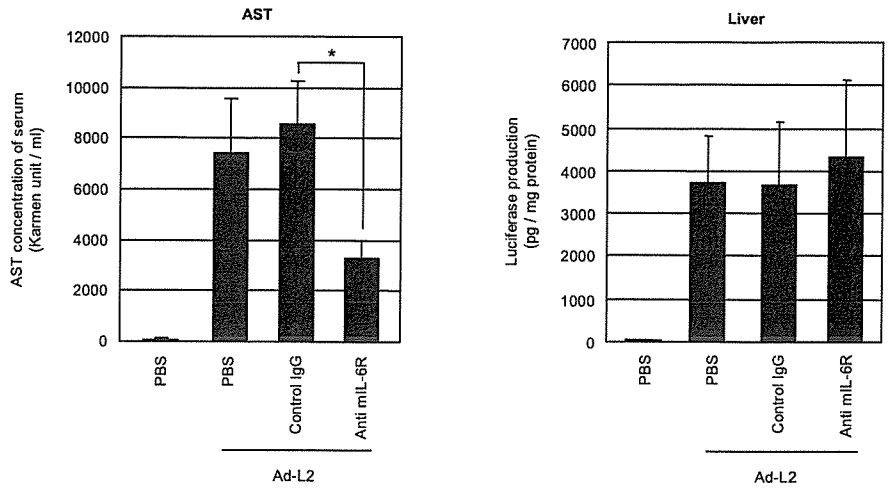

FIGURE 5. Effects of serum IL-6 on serum AST levels and liver luciferase production after the systemic administration of Ad-L2 into mice. C57BL/6 mice were i.p. administered 100 μg per mouse of anti-IL-6R Ab (clone D7715A7), which was specific for blocking IL-6 signaling, or rabbit IgG as a control (clone; R3-34). Ad-L2 or AdK7-L2 (3.0×10^{10} VP) was i.v. injected into the mice 1.5 h later. Blood samples and liver tissue were collected 48 h after the injection of Ad-L2. The AST levels in the serum were measured using a Transaminase-CII kit. Luciferase production in the liver was measured by a luciferase assay system. All data represent the means $\pm$ SD of three to four mice. *, $p < 0.01$.

after i.v. Ad administration is poorly understood. In the present study, although AdK7-L2 mediated higher luciferase expression and a higher accumulation of viral DNA in the liver than Ad-L2, it remains unclear why AdK7-L2 showed almost background levels of liver toxicity while Ad-L2 showed high toxicity. As reported previously, inflammatory cytokines, chemokines, and IFNs could be the mediators responsible for liver toxicity (2). IL-6 levels in the serum were the most strikingly different between AdK7-L2 and Ad-L2. Furthermore, IL-6 stimulated acute phase protein (serum amyloid A, fibrinogen, α_1-anti-trypsin, and α_1-acid glycoprotein) in rat and human hepatocytes (36, 37). Therefore, we next examined the effects of serum IL-6 on liver toxicity (Fig. 5). To do this, we used an anti-IL-6R Ab that inhibits the signal through the IL-6 receptor. The IL-6 receptor system consists of two functional molecules, an 80-kDa ligand-binding chain (IL-6R) and a 130-kDa nonligand-binding but signal-transducing chain (gp130). The anti-IL-6R Ab blocks the binding of IL-6 to the IL-6R (38, 39). The anti-IL-6R Ab or the control Ab was i.p. injected 1.5 h before the injection of Ad-L2. The AST levels in the serum and luciferase production in the liver were determined 48 h later. Administration of anti-IL-6R Ab significantly (~2-fold) reduced Ad vector-mediated AST levels in the serum compared with PBS or the control Ab (Fig. 5*A*). Importantly, anti-IL-6R Ab injection did not interfere with luciferase production in the liver (Fig. 5*B*). These results suggest that IL-6 signaling is involved in liver toxicity after i.v. administration of an Ad vector.

Discussion

In this study we found that the fiber-modified Ad vector containing the K7 peptide, which has high affinity with heparin sulfate, shows much lower serum IL-6 and liver toxicity than the conventional Ad vector. This improved characteristic is likely involved with the reduced biodistribution of the vector to the spleen compared with that of the conventional Ad vector. RT-PCR analysis showed that the spleen, not the liver, is the major site of cytokine, chemokine, and IFN (IL-6, IL-12, TNF-α, RANTES, MIP-2, IFN-α, IFN-β, and IFN-γ) production and that splenic conventional DC are the major effector cells of the innate immune response (at least IL-6 and IL-12 production) after i.v. administration of Ad vectors. We also showed that IL-6 signaling is involved in part with liver toxicity in response to Ad vectors. Importantly, this fiber-modified Ad vector containing the K7 peptide maintained higher transduction efficiency in all the organs examined, and the liver transduction was higher than that of the conventional Ad vector. Although there have been some reports that modified Ad vectors such as the pegylated Ad vector (18–21), the Ad vector containing the Ad type 35 fiber shaft and knob (40), and the triple mutant Ad vector with ablation of CAR, α_v integrin, and HSG binding (22) show decreased innate immune response and liver toxicity, these types of vector lose their transduction activity in vivo. To our knowledge, this is the first report of an Ad vector that maintains high transduction efficiency in vivo with reduced toxicity.

The fiber-modified Ad vector containing the K7 peptide has been developed to overcome the limitations imposed by the CAR dependence of Ad infection. Expanded and efficient gene transfer has been reported based on the use of mutant fiber proteins containing a stretch of lysine residues (23–25). However, there has been no report on the difference in gene transfer activity and toxicity in vivo between the conventional Ad vector and the fiber-modified Ad vector containing the K7 peptide. We have demonstrated that the fiber-modified Ad vector containing the K7 peptide mediates ~6-fold higher mouse liver transduction in response to i.v. administration than the conventional Ad vector (Fig. 1*A*). The amounts of fiber-modified Ad vector DNA in the liver after i.v. administration were also 5-fold higher than those with the conventional Ad vector (Fig. 1*B*). It has been reported that the interaction between the Ad type 5 fiber and the HSG of a hepatocyte is involved in the accumulation in the mouse liver and the cynomolgus monkey liver of systemically administered Ad vectors (41, 42). This fiber-modified Ad vector might mediate more efficient gene transduction through a much higher affinity for HSG. In contrast, the amounts of fiber-modified Ad vector DNA in the spleen after i.v. administration were 56-fold lower than those of the conventional Ad vector (Fig. 1*B*). Biodistribution of viral DNA reflects the total of receptor-mediated uptake and nonspecific uptake. Luciferase production in the cells mainly reflects receptor-mediated uptake. We previously reported that most Ad DNAs are taken up in the liver nonparenchymal cells, not parenchymal cells, after i.v. administration (22). In this study, the conventional Ad vector would also be taken up in the macrophages and DC by nonspecific uptake, resulting in significantly higher Ad DNA and lower luciferase production in the spleen. In contrast, the fiber-modified Ad vector would be taken up more in the liver via receptor-mediated uptake and nonspecific uptake, resulting in significantly lower Ad DNA in the other organs, especially the spleen. Even though the amount of AdK7-L2 uptake in the spleen, heart, lung, and kidney was less than that of Ad-L2 uptake, the amount of receptor-mediated uptake in these organs would be similar between Ad-L2 and AdK7-L2, suggesting that these vectors showed similar levels of luciferase production in the organs other than the liver.

The initiation of inflammatory innate immune responses occurs after the systemic administration of Ad vectors to animals and humans, and this toxicity limits the utility of Ad vectors for gene therapy. Increased cytokine/chemokine production after the injection of Ad vectors has been reported to be due to the introduction of input Ad vectors to Kupffer cells in the liver and DC (15, 17, 43–46). Detailed analysis of the organs responsible for the expression of cytokines, chemokines, and IFNs by RT-PCR suggests that their production can mainly be attributed to spleen cells (especially splenic conventional DC), not liver cells (Figs. 3 and 4), which is consistent with the recent report of Bart et al. (47). Therefore, interference with spleen distribution of the Ad vector should provide a useful method for safer gene therapy.

TLRs, which are crucial to the recognition of pathogen-associated molecular patterns, are expressed on various types of immune cells including macrophages, DC, B cells, splenic types of T cells, and even on nonimmune cells such as fibroblasts and epithelial cells (48). For example, HSV and CMV (dsDNA virus) activate inflammatory cytokines and type I IFN secretion by the stimulation of TLR9 (49–53). The innate immune receptor to the Ad has not yet been identified. It has not even been determined whether TLRs are involved in Ad-mediated innate immune response in vivo, although it has been reported that TLR signals are not involved in the DC maturation induced by the Ad vector (46). As shown in Fig. 3*B*, cytokine production against the Ad vector occurred mainly in conventional DC. It is noted that the TLR9-mediated innate immunity responses to DNA virus are cell type-specific and limited to plasmacytoid DC (50). The unidentified sensor receptor(s) for double-stranded Ad DNA or Ad capsid protein in conventional DC might play a critical role in the expression of inflammatory cytokines/chemokines and type I IFN. Although we have previously reported that large amounts of conventional Ad vector accumulate in nonparenchymal cells, including Kupffer cells and liver sinusoidal (endothelial) cells (22, 54), the expression of mRNA of cytokines, chemokines, and IFNs in the liver was weak after administration of the Ad vector (Fig. 3*B*). A lack of putative sensor receptor(s) against Ad or the inability of sensor receptor(s) to recognize Ad due to the specific cellular disposition of Ad in Kupffer cells might result in a reduced production of cytokines/chemokines/IFNs in the liver.

Another interesting finding is that the fiber-modified Ad vector containing the K7 peptide showed almost background levels of AST activity, which reflects liver toxicity (Fig. 2*B*). Histological analysis supported this finding (Fig. 2*C*). Because the K7-modified Ad vector showed higher transgene activity and a higher accumulation of viral DNA into the liver (Fig. 1), the transduction and distribution of the vector into the liver did not participate in liver toxicity. The cytokines/chemokines play a major causative role in liver damage associated with systemic Ad infusion as well as in the induction of an antiviral immune response (2). Ad-induced cytokines/chemokines recruit immune effector cells (neutrophils, monocyte/macrophages, and NK cells) to Ad-transduced cells (mainly liver), resulting in acute hepatic toxicity. Shayakhmetov et al. (35) have reported that hepatocytes and Kupffer cells trigger IL-1 transcription in liver tissue after i.v. administration of Ad vectors and that interference of IL-1-signaling reduces liver toxicity. We speculated that IL-6 could be the main mediator for hepatic toxicity because IL-6 is one of the main cytokines in the early stages of inflammation, IL-6 production by the fiber-modified Ad vector was much reduced (approximately a quarter) compared with that by the conventional Ad vector, and all of the cytokines/chemokines/IFNs we examined (including IL-6) were mainly produced by the spleen, not the liver. Treatment of the anti-IL-6R Ab decreased liver toxicity (Fig. 5), suggesting that IL-6 plays at least some role in liver toxicity induced by systemic injection of the Ad vector. Because the AST levels were only partially reduced by the treatment with the anti-IL-6R Ab, another mechanism such as IL-1 signaling, rapid Kupffer cell death (55, 56), activation of the liver endothelium (55), or other factors might be involved in the liver toxicity. Nevertheless, it is attractive that the K7-modified Ad vector did not show liver toxicity despite the higher transduction efficiency and higher accumulation of the vector into the liver (probably Kupffer cells).

Our present study provides new insight into the cellular biological mechanism related to the innate immune response and liver toxicity against the systemically administered Ad vector. Modification of vector tropism should contribute to safe gene therapy procedures.

Acknowledgments

We thank Misae Nishijima and Haiying Huang for their technical assistance.

Disclosures

The authors have no financial conflict of interest.

References

1. Muruve, D. A. 2004. The innate immune response to adenovirus vectors. *Hum. Gene Ther.* 15: 1157–1166.
2. Nazir, S. A., and J. P. Metcalf. 2005. Innate immune response to adenovirus. *J. Investig. Med.* 6: 292–304.
3. Yang, Y., H. C. Ertl, and J. M. Wilson. 1994. MHC class I-restricted cytotoxic T lymphocytes to viral antigens destroy hepatocytes in mice infected with E1-deleted recombinant adenoviruses. *Immunity* 1: 433–442.
4. Yang, Y., F. A. Nunes, K. Berencsi, E. E. Furth, E. Gonczol, and J. M. Wilson. 1994. Cellular immunity to viral antigens limits E1-deleted adenoviruses for gene therapy. *Proc. Natl. Acad. Sci. USA* 91: 4407–4411.
5. Yang, Y., Q. Su, and J. M. Wilson. 1996. Role of viral antigens in destructive cellular immune responses to adenovirus vector-transduced cells in mouse lungs. *J. Virol.* 70: 7209–7212.
6. Morral, N., R. J. Parks, H. Zhou, L. C. G. Schiedner, J. Quinones, F. L. Graham, S. Kochanek, and A. L. Beaudet. 1998. High doses of a helper-dependent adenoviral vector yield supraphysiological levels of α_1-antitrypsin with negligible toxicity. *Hum. Gene Ther.* 9: 2709–2716.
7. Morsy, M. A., M. Gu, S. Motzel, J. Zhao, J. Lin, Q. Su, H. Allen, L. Franlin, R. J. Parks, F. L. Graham, S. Kochanek, A. J. Bett, and C. T. Caskey. 1998. An adenoviral vector deleted for all viral coding sequences results in enhanced safety and extended expression of a leptin transgene. *Proc. Natl. Acad. Sci. USA* 95: 7866–7871.
8. Schiedner, G., N. Morral, R. J. Parks, Y. Wu, S. C. Koopmans, C. Langston, F. L. Graham, A. L. Beaudet, and S. Kochanek. 1998. Genomic DNA transfer with a high-capacity adenovirus vector results in improved in vivo gene expression and decreased toxicity. *Nat. Genet.* 18: 180–183.
9. Roberts, D. M., A. Nanda, M. J. Havenga, P. Abbink, D. M. Lynch, B. A. Ewald, J. Liu, A. R. Thorner, P. E. Swanson, D. A. Gorgone, et al. 2006. Hexon-chimaeric adenovirus serotype 5 vectors circumvent pre-existing anti-vector immunity. *Nature* 441: 239–243.
10. Farina, S. F., G. P. Gao, Z. Q. Xiang, J. J. Rux, R. M. Burnett, M. R. Alvira, J. Marsh, H. C. Ertl, and J. M. Wilson. 2001. Replication-defective vector based on a chimpanzee adenovirus. *J. Virol.* 75: 11603–11613.
11. Sakurai, F., H. Mizuguchi, and T. Hayakawa. 2003. Efficient gene transfer into human CD34$^+$ cells by an adenovirus type 35 vector. *Gene Ther.* 10: 1041–1048.
12. Vogels, R., D. Zuijdgeest, R. van Rijnsoever, E. Hartkoorn, I. Damen, M. P. de Bethune, S. Kostense, G. Penders, N. Helmus, W. Koudstaal, et al. 2003. Replication-deficient human adenovirus type 35 vectors for gene transfer and vaccination: efficient human cell infection and bypass of preexisting adenovirus immunity. *J. Virol.* 77: 8263–8271.
13. Holterman, L., R. Vogels, R. van der Vlugt, M. Sieuwerts, J. Grimbergen, J. Kaspers, E. Geelen, E. van der Helm, A. Lemckert, G. Gillissen, et al. 2004. Novel replication-incompetent vector derived from adenovirus type 11 (Ad11) for vaccination and gene therapy: low seroprevalence and non-cross-reactivity with Ad5. *J. Virol.* 78: 13207–13215.
14. Liu, Q., and D. A. Muruve. 2003. Molecular basis of the inflammatory response to adenovirus vectors. *Gene Ther.* 10: 935–940.
15. Zhang, Y., N. Chirmule, G. P. Gao, R. Qian, M. Croyle, B. Joshi, J. Tazelaar, and J. M. Wilson. 2001. Acute cytokine response to systemic adenoviral vectors in mice is mediated by dendritic cells and macrophages. *Mol. Ther.* 3: 697–707.
16. Clesham, G. J., P. J. Adam, D. Proudfoot, P. D. Flynn, S. Efstathiou, and P. L. Weissberg. 1998. High adenoviral loads stimulate NF-κB-dependent gene expression in human vascular smooth muscle cells. *Gene Ther.* 5: 174–180.
17. Lieber, A., C. Y. He, L. Meuse, D. Schowalter, I. Kirillova, B. Winther, and M. A. Kay. 1997. The role of Kupffer cell activation and viral gene expression in early liver toxicity after infusion of recombinant adenovirus vectors. *J. Virol.* 71: 8798–8807.

18. O'Riordan, C. R., A. Lachapelle, C. Delgado, V. Parkes, S. C. Wadsworth, A. E. Smith, and G. E. Francis. 1999. PEGylation of adenovirus with retention of infectivity and protection from neutralizing antibody in vitro and in vivo. *Hum. Gene Ther.* 10: 1349–1358.
19. Croyle, M. A., Q. C. Yu, and J. M. Wilson. 2000. Development of a rapid method for the PEGylation of adenoviruses with enhanced transduction and improved stability under harsh storage conditions. *Hum. Gene Ther.* 11: 1713–1722.
20. Croyle, M. A., H. T. Le, K. D. Linse, V. Cerullo, G. Toietta, A. Beaudet, and L. Pastore. 2005. PEGylated helper-dependent adenoviral vectors: highly efficient vectors with an enhanced safety profile. *Gene Ther.* 12: 579–587.
21. Mok, H., D. J. Palmer, P. Ng, and M. A. Barry. 2005. Evaluation of polyethylene glycol modification of first-generation and helper-dependent adenoviral vectors to reduce innate immune responses. *Mol. Ther.* 11: 66–79.
22. Koizumi, N., K. Kawabata, F. Sakurai, Y. Watanabe, T. Hayakawa, and H. Mizuguchi. 2006. Modified adenoviral vectors ablated for coxsackievirus-adenovirus receptor, α_v integrin, and heparan sulfate binding reduce in vivo tissue transduction and toxicity. *Hum. Gene Ther.* 17: 264–279.
23. Wickham, T. J., E. Tzeng, L. L. Shears II, P. W. Roelvink, Y. Li, G. M. Lee, D. E. Brough, A. Lizonova, and I. Kovesdi. 1997. Increased in vitro and in vivo gene transfer by adenovirus vectors containing chimeric fiber proteins. *J. Virol.* 11: 8221–8229.
24. Bouri, K., W. G. Feero, M. M. Myerburg, T. J. Wickham, I. Kovesdi, E. P. Hoffman, and P. R. Clemens. 1999. Polylysine modification of adenoviral fiber protein enhances muscle cell transduction. *Hum. Gene Ther.* 10: 1633–1640.
25. Koizumi, N., H. Mizuguchi, N. Utoguchi, Y. Watanabe, and T. Hayakawa. 2003. Generation of fiber-modified adenovirus vectors containing heterologous peptides in both the HI loop and C terminus of the fiber knob. *J. Gene Med.* 5: 267–276.
26. Mizuguchi, H., N. Koizumi, T. Hosono, N. Utoguchi, Y. Watanabe, M. A. Kay, and T. Hayakawa. 2001. A simplified system for constructing recombinant adenoviral vectors containing heterologous peptides in the HI loop of their fiber knob. *Gene Ther.* 8: 730–735.
27. Maizel, J. V., D. O. White, and M. D. Scharff. 1968. The polypeptides of adenovirus. I. Evidence for multiple protein components in the virion and a comparison of types 2, 7A, and 12. *Virology* 36: 115–125.
28. Xu, Z.-L., H. Mizuguchi, A. Ishii-Watabe, E. Uchida, T. Mayumi, and T. Hayakawa. 2001. Optimization of transcriptional regulatory elements for constructing plasmid vectors. *Gene* 272: 149–156.
29. Huard, J., H. Lochmuller, G. Acsadi, A. Jani, B. Massie, and G. Karpati. 1995. The route of administration is a major determinant of the transduction efficiency of rat tissues by adenoviral recombinants. *Gene Ther.* 2: 107–115.
30. Wood, M., P. Perrotte, E. Onishi, M. E. Harper, C. Dinney, L. Pagliaro, and D. R. Wilson. 1999. Biodistribution of an adenoviral vector carrying the luciferase reporter gene following intravesical or intravenous administration to a mouse. *Cancer Gene Ther.* 6: 367–372.
31. Worgall, S., G. Wolff, E. Falck-Pedersen, and R. G. Crystal. 1997. Innate immune mechanisms dominate elimination of adenoviral vectors following in vivo administration. *Hum. Gene Ther.* 8: 37–44.
32. Liu, Q., A. K. Zaiss, P. Colarusso, K. Patel, G. Haljan, T. J. Wickham, and D. A. Muruve. 2003. The role of capsid-endothelial interactions in the innate immune response to adenovirus vectors. *Hum. Gene Ther.* 14: 627–643.
33. Schiedner, G., S. Hertel, M. Johnston, V. Dries, R. N. Van, and S. Kochanek. 2003. Selective depletion or blockade of Kupffer cells leads to enhanced and prolonged hepatic transgene expression using high-capacity adenoviral vectors. *Mol. Ther.* 7: 35–43.
34. Engler, H., T. Machemer, J. Philopena, S. F. Wen, E. Quijano, M. Ramachandra, V. Tsai, and R. Ralston. 2004. Acute hepatotoxicity of oncolytic adenoviruses in mouse models is associated with expression of wild-type E1a and induction of TNF-α. *Virology* 328: 52–61.
35. Shayakhmetov, D. M., Z. Y. Li, S. Ni, and A. Lieber. 2005. Interference with the IL-1-signaling pathway improves the toxicity profile of systemically applied adenovirus vectors. *J. Immunol.* 174: 7310–7319.
36. Castell, J. V., T. Geiger, V. Gross, T. Andus, E. Walter, T. Hirano, T. Kishimoto, and P. C. Heinrich. 1988. Plasma clearance, organ distribution and target cells of interleukin-6/hepatocyte-stimulating factor in the rat. *Eur. J. Biochem.* 177: 357–361.
37. Geiger, T., T. Andus, J. Klapproth, T. Hirano, T. Kishimoto, and P. C. Heinrich. 1988. Induction of rat acute-phase proteins by interleukin 6 in vivo. *Eur. J. Immunol.* 18: 717–721.
38. Vink, A., P. Coulie, G. Warnier, J. C. Renauld, M. Stevens, D. Donckers, and J. Van Snick. 1990. Mouse plasmacytoma growth in vivo: enhancement by interleukin 6 (IL-6) and inhibition by antibodies directed against IL-6 or its receptor. *J. Exp. Med.* 172: 997–1000.
39. Boulanger, M. J., D. C. Chow, E. E. Brevnova, and K. C. Garcia. 2003. Hexameric structure and assembly of the interleukin-6/IL-6 α-receptor/gp130 complex. *Science* 300: 2101–2104.
40. Shayakhmetov, D. M., Z. Y. Li, S. Ni, and A. Lieber. 2004. Analysis of adenovirus sequestration in the liver, transduction of hepatic cells, and innate toxicity after injection of fiber-modified vectors. *J. Virol.* 78: 5368–5381.
41. Smith, T. A., N. Idamakanti, M. L. Rollence, J. Marshall-Neff, J. Kim, K. Mulgrew, G. R. Nemerow, M. Kaleko, and S. C. Stevenson. 2003. Adenovirus serotype 5 fiber shaft influences in vivo gene transfer in mice. *Hum. Gene Ther.* 14: 777–787.
42. Smith, T. A., N. Idamakanti, J. Marshall-Neff, M. L. Rollence, P. Wright, M. Kaloss, L. King, C. Mech, L. Dinges, W. O. Iverson, et al. 2003. Receptor interactions involved in adenoviral-mediated gene delivery after systemic administration in non-human primates. *Hum. Gene Ther.* 14: 1595–1604.
43. Schnell, M. A., Y. Zhang, J. Tazelaar, G. P. Gao, Q. C. Yu, R. Qian, S. J. Chen, A. N. Varnavski, C. LeClair, S. E. Raper, and J. M. Wilson. 2001. Activation of innate immunity in nonhuman primates following intraportal administration of adenoviral vectors. *Mol. Ther.* 3: 708–722.
44. Morral, N., W. K. O'Neal, K. M. Rice, P. A. Piedra, E. Aguilar-Cordova, K. D. Carey, A. L. Beaudet, and C. Langston. 2002. Lethal toxicity, severe endothelial injury, and a threshold effect with high doses of an adenoviral vector in baboons. *Hum. Gene Ther.* 13: 143–154.
45. Reid, T., E. Galanis, J. Abbruzzese, D. Sze, L. M. Wein, J. Andrews, B. Randlev, C. Heise, M. Uprichard, M. Hatfield, et al. 2002. Hepatic arterial infusion of a replication-selective oncolytic adenovirus (dl1520): phase II viral, immunologic, and clinical endpoints. *Cancer Res.* 62: 6070–6079.
46. Philpott, N. J., M. Nociari, K. B. Elkon, and E. Falck-Pedersen. 2004. Adenovirus-induced maturation of dendritic cells through a PI3 kinase-mediated TNF-α induction pathway. *Proc. Natl. Acad. Sci. USA* 1001: 6200–6205.
47. Bart, D. G., S. Jan, V. L. Sophie, L. Joke, and C. Desire. 2005. Elimination of innate immune responses and liver inflammation by PEGylation of adenoviral vectors and methylprednisolone. *Hum. Gene Ther.* 16: 1439–1451.
48. Akira, S., S. Uematsu, and O. Takeuchi. 2006. Pathogen recognition and innate immunity. *Cell* 124: 783–801.
49. Lund, J., A. Sato, S. Akira, R. Medzhitov, and A. Iwasaki. 2003. Toll-like receptor 9-mediated recognition of herpes simplex virus-2 by plasmacytoid dendritic cells. *J. Exp. Med.* 198: 513–520.
50. Hochrein, H., B. Schlatter, M. O'Keeffe, C. Wagner, F. Schmitz, M. Schiemann, S. Bauer, M. Suter, and H. Wagner. 2004. Herpes simplex virus type-1 induces IFN-α production via Toll-like receptor 9-dependent and -independent pathways. *Proc. Natl. Acad. Sci. USA* 101: 11416–11421.
51. Krug, A., A. R. French, W. Barchet, J. A. Fischer, A. Dzionek, J. T. Pingel, M. M. Orihuela, S. Akira, W. M. Yokoyama, and M. Colonna. 2004. TLR9-dependent recognition of MCMV by IPC and DC generates coordinated cytokine responses that activate antiviral NK cell function. *Immunity* 21: 107–119.
52. Krug, A., G. D. Luker, W. Barchet, D. A. Leib, S. Akira, and M. Colonna. 2004. Herpes simplex virus type 1 activates murine natural interferon-producing cells through toll-like receptor 9. *Blood* 103: 1433–1437.
53. Tabeta, K., P. Georgel, E. Janssen, X. Du, K. Hoebe, K. Crozat, S. Mudd, L. Shamel, S. Sovath, J. Goode, et al. 2004. Toll-like receptors 9 and 3 as essential components of innate immune defense against mouse cytomegalovirus infection. *Proc. Natl. Acad. Sci. USA* 101: 3516–3521.
54. Koizumi, N., H. Mizuguchi, F. Sakurai, T. Yamaguchi, Y. Watanabe, and T. Hayakawa. 2003. Reduction of natural adenovirus tropism to mouse liver by fiber-shaft exchange in combination with both CAR- and α_v integrin-binding ablation. *J. Virol.* 24: 13062–13072.
55. Schiedner, G., W. Bloch, S. Hertel, M. Johnston, A. Molojavyi, V. Dries, G. Varga, N. Van Rooijen, and S. Kochanek. 2003. A hemodynamic response to intravenous adenovirus vector particles is caused by systemic Kupffer cell-mediated activation of endothelial cells. *Hum. Gene Ther.* 14: 1631–1641.
56. Manickan, E., J. S. Smith, J. Tian, T. L. Eggerman, J. N. Lozier, J. Muller, and A. P. Byrnes. 2006. Rapid Kupffer cell death after intravenous injection of adenovirus vectors. *Mol. Ther.* 13: 108–117.

Gene Therapy (2007), 1–12

www.nature.com/gt

ORIGINAL ARTICLE

Cotransduction of CCL27 gene can improve the efficacy and safety of IL-12 gene therapy for cancer

J-Q Gao[1,5,6], N Kanagawa[1,6], Y Motomura[1], T Yanagawa[1], T Sugita[1], Y Hatanaka[2], Y Tani[2], H Mizuguchi[3], Y Tsutsumi[3], T Mayumi[4], N Okada[1] and S Nakagawa[1]

[1]*Department of Biotechnology and Therapeutics, Graduate School of Pharmaceutical Sciences, Osaka University, Suita, Osaka, Japan;* [2]*Department of Biomedical Science, Dako Japan Co., Ltd, Nishinotouin-higashiiru, Shijo-dori, Shimogyo-ku, Kyoto, Japan;* [3]*National Institute of Biomedical Innovation, Ibaraki, Osaka, Japan and* [4]*Kobe-gakuin University, Igawadani, Nishi-ku, Kobe, Japan*

Interleukin-12 (IL-12) is a potent antitumoral cytokine, but high doses are toxic. Herein, we demonstrate that combinational transduction of IL-12 and CC-chemokine ligand-27 (CCL27) genes into pre-existing murine OV-HM ovarian carcinoma and Meth-A fibrosarcoma, by using RGD fiber-mutant adenoviral vectors, could induce tumor regression and relieve systemic side effects more effectively than either treatment alone. The antitumor activity of the IL-12 and CCL27 combination treatment was T-cell-dependent, and development of long-term specific immunity was confirmed in rechallenge experiments. Immunohistochemical analysis of tumors transduced with CCL27 gene alone or cotransduced with IL-12 and CCL27 genes showed significant increases in numbers of infiltrating CD3⁺ T cells, which included both CD4⁺ and CD8⁺ cells. Additionally, cotransduction with IL-12 and CCL27 genes could more efficiently activate tumor-infiltrating immune cells than transduction with CCL27 alone, as determined by the frequency of perforin-positive cells and expression levels of IFN-γ. Furthermore, mice treated with the IL-12 and CCL27 combination compared with those treated with IL-12 alone showed milder pathological changes, for example, lymphocyte infiltration and extramedullary hematopoiesis, in lung, liver and spleen. Our data provide evidence that combinational in vivo *transduction with IL-12 and CCL27 genes is a promising approach for the development of cancer immunogene therapy that can simultaneously recruit and activate tumor-infiltrating immune cells.*

Gene Therapy advance online publication, 4 January 2007; doi:10.1038/sj.gt.3302892

Keywords: *IL-12; CCL27; cancer immunogene therapy; adenovirus; tumor-infiltrating immune cell*

Introduction

Multifunctional cytokine interleukin-12 (IL-12) is a 70 kDa (p70) heterodimeric protein in which the 40 kDa (p40) and 35 kDa (p35) subunits are connected by one disulfide bond.[1,2] IL-12 is mainly secreted by antigen-presenting cells including dendritic cells (DCs) and macrophages and is known for its antitumor properties, effected through the induction of specific cellular immune responses, such as the enhancement of proliferative and cytotoxic activities of natural killer (NK) cells and cytotoxic T lymphocytes (CTLs),[3,4] the production of interferon-γ (IFN-γ) from activated cells,[4–6] and the promotion of helper T type 1 (Th1) cell differentiation from Th0 cells.[4,7,8] IFN-γ is involved in IL-12-mediated tumor regression,[9] and IL-12 also exhibits an antiangiogenic effect that can account for some antitumor activity.[10] Although recombinant IL-12 administration at high doses is effective for cancer treatment, major drawbacks of this therapy are the serious adverse effects associated with high systemic peak IL-12 concentrations.[11,12] Moreover, even in gene therapy aiming for persistent local IL-12 expression by using intratumoral injection of a vector carrying the IL-12 gene, careful evaluation of the vector dosage is required to restrict IL-12 leakage from the tumor tissue to the systemic blood circulation.[13] Therefore, in order to realize clinical applications of IL-12–based cancer therapy, we need to explore innovative approaches that can elicit more effective tumor immunity at IL-12 doses lower than the maximum tolerance dosage.

On the basis of the relative benefits and risks of IL-12 for cancer treatment, we hypothesized that if small amounts of IL-12 can efficiently and persistently act on a large number of immune cells only within the local tumor tissue, such IL-12-based cancer immunotherapy may suppress adverse effects while maintaining excellent tumor immunity inducibility. However, it is known that infiltration of immune cells is generally hard to achieve in tumor tissue, and that several tumor models, such as Meth-A and MCH-1A1 tumors, are resistant to treatment with systemically administered IL-12 specifically due to poor tumor infiltration of lymphocytes.[14,15] In addition, because conventional cancer immunotherapy research, involving the development of various vaccine strategies, has mainly focused on efficient

Correspondence: Dr N Okada or Professor S Nakagawa, Department of Biotechnology and Therapeutics, Graduate School of Pharmaceutical Sciences, Osaka University, 1-6 Yamadaoka, Suita, Osaka 565-0871, Japan.
E-mails: okada@phs.osaka-u.ac.jp or nakagawa@phs.osaka-u.ac.jp.
[5]Current address: Institute of Pharmaceutics, Zhejiang University, 353 Yan-an Road, Hangzhou 310031, PR China.
[6]These authors contributed equally to this work.
Received 16 June 2006; revised 26 September 2006; accepted 3 November 2006

induction and activation of the host's immune response to tumors, the methodology that can adequately recruit immune cells into tumor tissue is not yet established. In order to better control trafficking and biodistribution of immune cells in cancer immunotherapy, we and several other groups recently proposed novel strategies based on the application of chemokine-chemokine receptor coupling.[16–23]

Chemokines, which are small (8–14 kDa), basic, secreted proteins, regulate leukocytic migration and infiltration of local sites through cooperation with various cell adhesion molecules.[24] To date, more than 50 chemokines have been identified, and they compose a superfamily that contains four subgroups: C-chemokine, CC-chemokine, CXC-chemokine and CX3C-chemokine.[25] Within this superfamily, immune chemokines, which primarily target lymphocytes and DCs, would be useful molecules to improve the efficacy of cancer immunotherapy by augmenting tumor-infiltrating immune cells. We previously reported that tumorigenicity of the murine ovarian carcinoma cell line, OV-HM cells, was attenuated through enhanced tumor-infiltration by immune cells including NK and T cells, effected via *in vitro* transfection with CC-chemokine ligand-27 (CCL27) using RGD-fiber mutant adenoviral vector (AdRGD).[21] Although 70% of mice inoculated with CCL27-transfected OV-HM cells achieved complete rejection, these mice exhibited only limited long-term immunity in OV-HM-rechallenged experiments. Our results suggested that the tumor-infiltrating immune cells attracted by CCL27 gene transduction should be activated in a tumor-specific manner in order to induce more effective tumor immunity. In addition, because the *ex vivo* approach is not applicable for clinical use in patients with established malignant disease, we need to analyze both antitumor efficacy and activation state of tumor-infiltrating immune cells on direct *in vivo* transduction models using AdRGD-CCL27 plus other immunomodulators. Hence, a combinational therapy using IL-12- and CCL27-expressing vectors at low doses, for example, could potentially provide enhanced antitumor activity and long-term immune responses through the effective recruitment and activation of tumor-infiltrating immune cells, without the serious adverse effects of IL-12 leakage into the systemic circulation.

Thus, in the present study using the established murine OV-HM tumor (responsive to IL-12) and Meth-A tumor (unresponsive to IL-12) models, we compared intratumoral injections with AdRGD-IL12 alone, AdRGD-CCL27 alone, and the combination of AdRGD-IL12 and AdRGD-CCL27, in terms of tumor suppressive effects, frequency and activation state of tumor-infiltrating immune cells, as well as systemic adverse effects.

Results

Synergistic antitumor effects and long-term specific immune response induced by the combinational intratumoral injection of AdRGD-IL12 and AdRGD-CCL27

In order to evaluate the antitumoral effects of direct *in vivo* gene transduction in established OV-HM and Meth-A tumors, we investigated the changes in tumor size and the survival ratios of mice tested after intratumoral injection with various combinations of AdRGDs. We utilized a total vector dosage of 2×10^7 PFU (plaque-forming unit) in the therapeutic experiments based on our observations that any group, including mice injected intratumorally with AdRGD-IL12 alone, did not show severe adverse effects, such as body weight reduction and sudden death, at dosages lower than this level (data not shown).

As shown in Figure 1a, OV-HM tumors injected with luciferase-expressing AdRGD (AdRGD-Luc; control vector) showed delayed growth compared with that of vehicle-injected tumors, and the growth of OV-HM tumors injected with AdRGD-CCL27 alone was nearly equal to that of AdRGD-Luc-injected tumors. These results suggested that OV-HM tumors were easily injured by direct *in vivo* transduction with AdRGDs, and that their growth was not affected by only CCL27 gene transduction, at least in this therapeutic model. On the other hand, intratumoral injection of AdRGD-IL12 alone induced obvious suppressive effects on OV-HM tumor growth, and even achieved complete regression in 4 of 7 mice (Figure 1b). Although the survival ratio in mice treated with AdRGD-IL12 alone improved with increased vector dosage, there were also higher numbers of mice exhibiting body weight reduction (data not shown). Therefore, we examined whether the combination of AdRGD-IL12 and AdRGD-CCL27 could induce any synergistic effects for inhibition of OV-HM tumor growth without any concomitant side effects. Intratumoral co-injection of AdRGD-IL12 and AdRGD-CCL27 in a total vector dose ratio of 1:1 showed better antitumor effects than injection with AdRGD-IL12 alone, whereas treatment with AdRGD-IL12 and AdRGD-CCL27 in a ratio of 1:9 was ineffective compared with injection with AdRGD-CCL27 alone. Importantly, all mice treated with co-injection of AdRGD-IL12 and AdRGD-CCL27 in a vector dose ratio of 9:1 achieved complete regression of the primary tumor and survived more than 3 months after treatment without any severe adverse effects, such as body weight reduction and sudden death. In the established Meth-A tumor model, intratumoral injection of AdRGD-Luc alone or AdRGD-CCL27 alone did not affect tumor growth and survival ratio as compared with phosphate-buffered saline (PBS)-administration (Figure 1c and d). Although Meth-A tumors injected with AdRGD-IL12 alone showed marked regression, the combination of AdRGD-IL12 and AdRGD-CCL27 in a vector ratio of 9:1 produced very strong antitumor effects, similar to those seen in the OV-HM tumor model. Furthermore, most of the mice which achieved complete regression of primary tumors by the combination of AdRGD-IL12 and AdRGD-CCL27 in a ratio of 9:1 were also protected against rechallenge with the same tumor at 3 or 6 months after treatment (Table 1). In contrast, rechallenge of different tumor (B16BL6 or CT26) of which haplotype matched to recipient induced palpable tumor formation in all primary tumor-regressed mice within 2 weeks, indicating that the systemic long-term immunity generated in mice receiving the AdRGD-IL12 and AdRGD-CCL27 combinational therapy was specific for primary tumors (OV-HM or Meth-A).

Taken together, these results clearly revealed that the combination of low doses AdRGD-CCL27 could synergistically enhance the efficacy of IL-12 gene therapy for

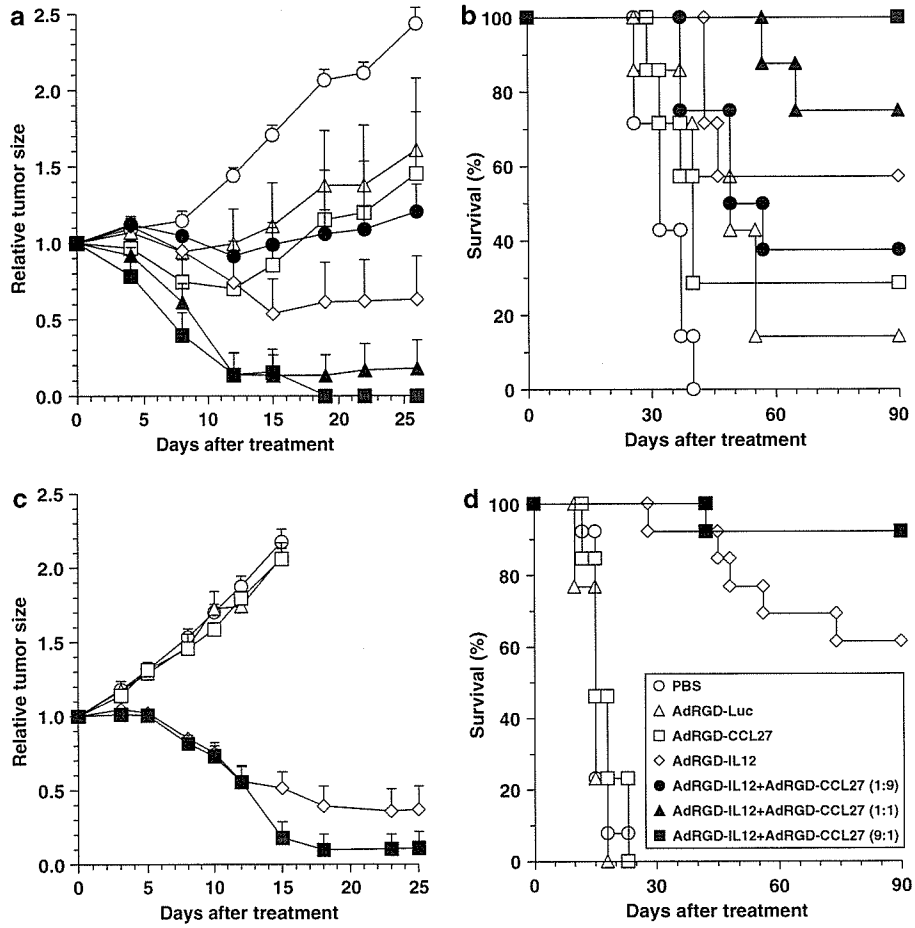

Figure 1 Antitumor efficacy of intratumorally injected AdRGD-IL12 plus AdRGD-CCL27 in OV-HM or Meth-A tumor model. B6C3F1 mice (**a** and **b**) or BALB/c mice (**c** and **d**) were intradermally inoculated with 10^6 OV-HM cells or 2×10^6 Meth-A cells, respectively, into the flanks. The tumors (7–9 mm in diameter) were injected with either AdRGD-Luc alone, AdRGD-IL12 alone, AdRGD-CCL27 alone, or the combination of AdRGD-IL12 and AdRGD-CCL27 in a ratio of 1:9, 1:1 or 9:1 at the same dose totaling 2×10^7 PFU. PBS was injected into the tumors as a control. (**a** and **c**) The sizes of growing tumors were measured twice or three times a week using microcalipers. The data were expressed as a relative tumor size to the initial (day 0) tumor size. Each point represents the mean ± s.e. of results from seven or eight mice. (**b** and **d**) Data represent the number of mice for which tumors were smaller than 20 mm, expressed as a percentage of the total mice tested in each group.

OV-HM and Meth-A tumors, and that the antitumor responses were both specific and long lasting.

Subset of immune cells responsible for antitumor efficacy of the combination of AdRGD-IL12 and AdRGD-CCL27

Next, in order to elucidate whether T-cell functions were involved in the induction of the observed antitumor effects, we carried out therapeutic protocols with intratumoral co-injection of AdRGD-IL12 and AdRGD-CCL27 in a ratio of 9:1 totaling 2×10^7 PFU against established OV-HM and Meth-A tumors in BALB/c nude mice (data not shown). The AdRGD-IL12 and AdRGD-CCL27 combinational treatment was not able to restrain growth of OV-HM tumors established in nude mice. Although growth of Meth-A tumors was slightly delayed in nude mice treated with the AdRGD-IL12 and AdRGD-CCL27 combination, there were no individuals demonstrating tumor regression, unlike the experiments with immunocompetent mice. These results confirmed that tumor regression by the intratumoral co-injection with AdRGD-IL12 and AdRGD-CCL27 was mainly based on a T-cell-dependent immune response.

In addition, we performed *in vivo* depletion analysis using specific antibodies against CD4, CD8 and asialoGM1 in the OV-HM and Meth-A tumor model. As shown in Figure 2a, anti-OV-HM tumor effects of the combination of AdRGD-IL12 and AdRGD-CCL27 were attenuated by depletion of $CD8^+$ T cells, $CD4^+$ T cells and NK cells in B6C3F1 mice, with CD8-depletion being the most effective at abrogating the therapeutic effects. Moreover, OV-HM tumors in mice with depletion of both $CD4^+$ and $CD8^+$ T cells, in spite of treatment with AdRGD-IL12 and AdRGD-CCL27, showed more enhanced growth than those in mice with PBS-administration. On the other hand, growth suppressive effects of AdRGD-IL12 and AdRGD-CCL27 combinational therapy against Meth-A tumors were not affected by $CD4^+$ T cell depletion, whereas the depletion of $CD8^+$ T cells, NK cells and both $CD4^+$ and $CD8^+$ T cells attenuated antitumor effects, similar to the pattern shown in OV-HM tumor model (Figure 2b). Therefore, we concluded that $CD8^+$ CTLs, which were activated by the helper function of $CD4^+$ T cells, were the predominant effector

Table 1 Induction of long-term specific immunity in mice that could achieve complete regression of the primary tumor by intratumoral injection with the combination of AdRGD-IL12 and AdRGD-CCL27

Strain	*Groups*	*Rechallenging cells*	*Tumor rejected mice/tested mice*		
			Exp. 1[a]	*Exp. 2*[a]	*Exp. 3*[b]
B6C3F1	Intact mice	OV-HM[c]	0/6	0/6	0/6
	OV-HM-regressed mice	OV-HM[c]	4/5	5/5	5/5
	OV-HM-regressed mice	B16BL6[d]	0/3	0/5	0/5
BALB/c	Intact mice	Meth-A[e]	0/10	—	—
	Meth-A-regressed mice	Meth-A[e]	12/12	—	—
	Meth-A-regressed mice	CT26[f]	0/5	—	—

[a]Tumor challenge was performed 3 months after treatment with the combination of AdRGD-IL12 and AdRGD-CCL27 in a ratio of 9:1 at a total of 2×10^7 PFU.
[b]Tumor challenge was performed 6 months after treatment with the combination of AdRGD-IL12 and AdRGD-CCL27 in a ratio of 9:1 at total of 2×10^7 PFU.
[c]OV-HM cells were inoculated at 10^6 cells/mouse.
[d]B16BL6 cells were inoculated at 3×10^5 cells/mouse.
[e]Meth A cells were inoculated at 10^6 cells/mouse.
[f]CT26 cells were inoculated at 3×10^5 cells/mouse.

cells in our therapeutic experiments, although the cytotoxic activity of NK cells also partly contributed to the enhanced antitumor effects seen with intratumoral co-injection of AdRGD-IL12 and AdRGD-CCL27.

The subset and activation state of infiltrating T cells in OV-HM and Meth-A tumors co-injected with AdRGD-IL12 and AdRGD-CCL27

We attempted to identify, by immunohistochemical analysis, the subset of infiltrating T cells in OV-HM and Meth-A tumors 6 days after injection of the combination of AdRGD-IL12 and AdRGD-CCL27 in a ratio of 9:1 totaling 2×10^7 PFU. In comparison with PBS-injected tumors, tumors injected with AdRGD-Luc exhibited nearly equal numbers of infiltrating $CD3^+$ T cells in both tumor models (Figure 4a and b), indicating that intratumoral administration of AdRGD at 2×10^7 PFU did not influence T-cell accumulation. Notably, a large number of $CD3^+$ T cells were detected in tumors co-injected with AdRGD-IL12 and AdRGD-CCL27 as well as in tumors injected with AdRGD-CCL27 alone (Figures 3a and b, and 4a and b). OV-HM tumors injected with AdRGD-IL12 alone showed a significantly smaller number of infiltrating $CD3^+$ T cells than those injected with AdRGD-CCL27 alone or AdRGD-IL12 plus AdRGD-CC27 (Figure 4a). In the Meth-A tumor model, although no differences in $CD3^+$ T-cell accumulation were observed between tumors injected with AdRGD-CCL27 alone and AdRGD-IL12 alone, the frequency of $CD3^+$ T cells in tumors treated with the combination of AdRGD-IL12 and AdRGD-CCL27 was slightly higher than that in tumors injected with each AdRGD alone (Figure 4b). In addition, subset analysis of tumor-infiltrating T cells revealed that co-injection of AdRGD-IL12 and AdRGD-CCL27 promoted infiltration into tumor tissue of both $CD4^+$ and $CD8^+$ subsets, composed of Th cells and CTLs respectively (Figures 3c–f and 4c–f). Injection of AdRGD-CCL27 alone induced a large number of infiltrating $CD4^+$ cells and a relatively small number of infiltrating $CD8^+$ cells in the OV-HM tumor model (Figure 4c and e). In contrast, the CCL27-induced infiltrating T cells were biased in favor of the $CD8^+$ subset rather than the $CD4^+$ subset in the Meth-A tumor model (Figure 4d and f). Although the cause of the resulting differences in CCL27-induced effects between both tumor types was unclear, these results suggest that the balance of immune cell subsets attracted by chemokines might be affected by different tumor tissue microenvironments. Collectively, intratumoral co-injection of AdRGD-IL12 and AdRGD-CCL27 more effectively augmented infiltration of both $CD4^+$ and $CD8^+$ T cell subsets in OV-HM and Meth-A tumor parenchyma than injection of AdRGD-IL12 alone.

Subsequently, we examined the activation states of tumor-infiltrating T cells by immunohistochemical analysis for perforin, which is the major cytotoxic molecule in activated CTLs. As shown in Figures 3g, 5a and b, few perforin-positive cells were detected in OV-HM or Meth-A tumors injected with AdRGD-Luc as well as in PBS-administered tumors. Similarly, the perforin-positive cells were hardly detectable in tumor-infiltrating T cells attracted by injection of AdRGD-CCL27 alone (Figure 5a and b), indicating that CCL27 did not significantly attract activated effector cells possessing potent tumor cell-killing activity. On the other hand, tumors injected with AdRGD-IL12 alone exhibited significantly higher numbers of perforin-positive cells than those injected with AdRGD-CCL27 alone. Importantly, compared with the AdRGD-IL12-treated group, tumor-infiltrating cells in a sensitized/activated state were more effectively augmented by the AdRGD-IL12 and AdRGD-CCL27 combinational treatment (Figures 3h, 5a and b). In addition, reverse transcription-polymerase chain reaction (RT-PCR) analysis using isolated total RNA from OV-HM tumors subjected to the various treatments, showed that PCR products derived from transcripts of IFN-γ, which are the secreted cytokines from IL-12-activated cells including Th1 cells and CTLs, were detected at high levels only in tumors injected with AdRGD-IL12 alone or AdRGD-IL12 plus AdRGD-CCL27 (Figure 5c). Furthermore, $CD4^+$ or $CD8^+$ T cells isolated from Meth-A tumors with the co-injection of AdRGD-IL12 and AdRGD-CCL27 contained more IFN-γ-producing cells than those

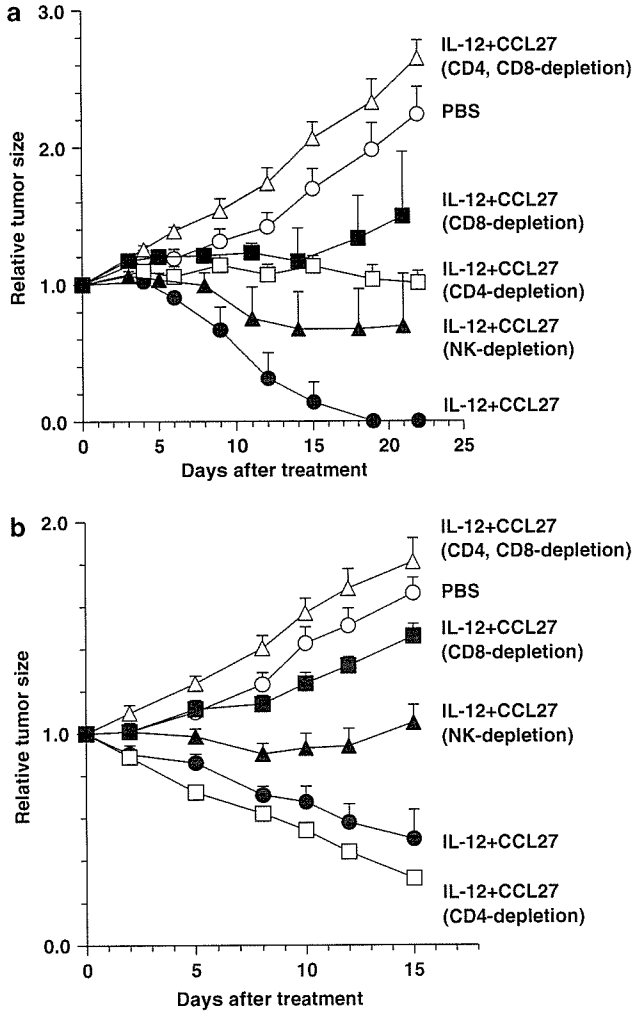

Figure 2 Determination of immune subsets responsible for the antitumor efficacy induced by the IL-12/CCL27 combination. On day −7, B6C3F1 mice (**a**) or BALB/c mice (**b**) were intradermally inoculated with 10^6 OV-HM cells or 2×10^6 Meth-A cells, respectively, into the flanks. For depletion of $CD4^+$ T cells, $CD8^+$ T cells or NK cells in the mice, GK1.5 ascites (anti-CD4), 53–6.72 ascites (anti-CD8) or anti-asialoGM1 antisera were intraperitoneally injected on days −3, −2, −1, 0, 5, 10 and 15. On day 0, OV-HM tumors received the IL-12/CCL27 combination intratumoral injection in a ratio of 9:1 totaling 2×10^7 PFU. The data were expressed as a relative tumor size to the initial (day 0) tumor size. Each point represents the mean ± s.e. of results from five to seven mice.

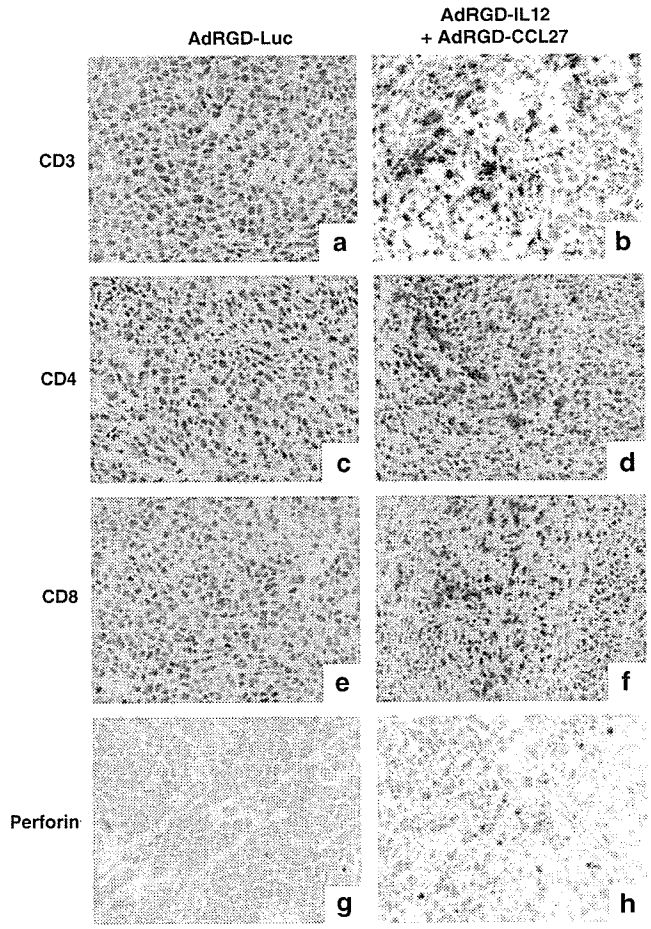

Figure 3 Images of infiltrating T cells in OV-HM tumors injected with the IL-12/CCL27 combination. OV-HM cells were intradermally inoculated into the flanks of B6C3F1 mice at 10^6 cells/mouse. The tumors (7–9 mm in diameter) were injected with AdRGD-Luc alone (**a**, **c**, **e** and **g**) or AdRGD-IL12 plus AdRGD-CCL27 in a ratio of 9:1 (**b**, **d**, **f** and **h**) at the same dose totaling 2×10^7 PFU. On day 6 after the intratumoral injections, immunohistochemical staining against CD3 (**a** and **b**), CD4 (**c** and **d**), CD8 (**e** and **f**) and perforin (**g** and **h**) was performed using frozen tumor sections. Original magnifications are × 400.

from tumors with other treatments in flow cytometric analysis (Figure 5d). These findings support the observation that tumors co-injected with AdRGD-IL12 and AdRGD-CCL27 could recruit activated T cells in higher frequency compared with tumors treated with AdRGD-IL12 alone or AdRGD-CCL27 alone.

Taken together, these data from immunohistochemical, RT-PCR and flow cytometric analyses demonstrate that the simultaneous production of IL-12 and CCL27 in tumor tissues could work synergistically, via the chemoattractant activity of CCL27 and the immunostimulating ability of IL-12, to expand the numbers of infiltrating T cells in an effector phase. Also, the frequencies of both perforin-positive cells and IFN-γ-producing T cells in tumor parenchyma correlated closely with differences in the antitumor effects (Figures 1 and 5), strongly suggesting that efficient accumulation of activated tumor-specific CTLs at a local tumor site is a key factor for establishment of efficacious cancer immunotherapy.

Reduction of adverse effects caused by IL-12 in the combinational therapy using AdRGD-IL12 and AdRGD-CCL27

In our therapeutic experiments, severe adverse effects including body weight reduction and sudden death were not observed in any treated mice. However, mice achieving complete regression of primary Meth-A tumor by treatment with AdRGD-IL12 alone showed some histopathological changes in the lung, liver and spleen. In all lungs collected from mice treated with AdRGD-IL12 alone, rare to moderate levels of lymphocyte infiltration into the perivascular lymph sinus were observed (Figure 6a and g), and hemorrhagic lesions were also often found. Also, microgranuloma, interstitial lymphocyte infiltration and extramedullary hematopoi-

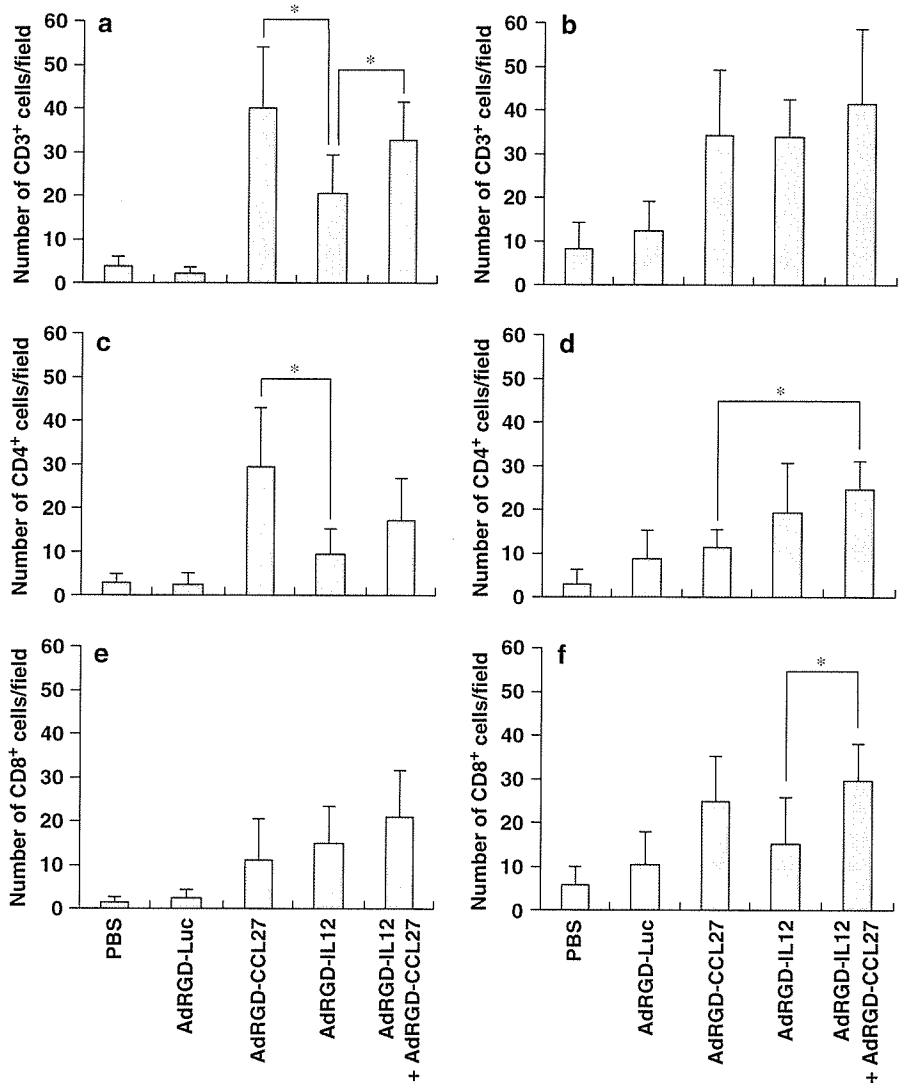

Figure 4 Quantification of tumor-infiltrating T-cell subsets in OV-HM and Meth-A tumors injected with the IL-12/CCL27 combination. OV-HM cells (**a**, **c** and **e**) or Meth-A cells (**b**, **d** and **f**) were intradermally inoculated into the flanks of syngeneic mice at 10^6 or 2×10^6 cells/mouse, respectively. The tumors (7–9 mm in diameter) were injected with AdRGD-Luc alone, AdRGD-IL12 alone, AdRGD-CCL27 alone, or the AdRGD-IL12 and AdRGD-CCL27 combination in a ratio of 9:1 at the same dose totaling 2×10^7 PFU. PBS was injected into the tumors as a control. On day 6 after the intratumoral injections, immunohistochemical staining against CD3, CD4 and CD8 was performed using frozen tumor sections. These immunohistochemical sections were used to assess the numbers of $CD3^+$ (**a** and **b**), $CD4^+$ (**c** and **d**) and $CD8^+$ (**e** and **f**) cells infiltrating into tumor parenchyma by counting six fields per specimen under $\times$ 400-magnification. The data represent the mean $\pm$ s.d. of results from three tumors. Statistical analysis was carried out using Welch's *t*-test: $^*P < 0.05$, $^{**}P < 0.01$.

esis were rarely observed in the livers from 4 of 6 mice (Figure 6b and g), and four of six specimens of spleen exhibited augmentation of extramedullary hematopoiesis (Figure 6c and g). On the other hand, in the group treated with the AdRGD-IL12 and AdRGD-CCL27 combination, the extramedullary hematopoiesis in the liver was not observed, whereas lymphocyte infiltration and lung hemorrhages were less evident compared with the group treated with AdRGD-IL12 alone (Figure 6d, e and g). In addition, the enhancement of extramedullary hematopoiesis was not observed in splenic examinations of mice treated with the AdRGD-IL12 and AdRGD-CCL27 combination (Figure 6f and g). These results indicate that IL-12 disseminated from local tumor sites into the systemic circulation might cause undesired histopathological changes in mice treated with AdRGD-IL12 alone, and that the combination of AdRGD-CCL27 at low doses was a promising approach for suppressing the adverse effects in IL-12 gene therapy for cancer.

Discussion

The development of cancer immunotherapy aims for sufficient induction of the tumor-specific immune responses to a level capable of tumor rejection and regression, and involves three criteria for the immunological elimination of established tumor mass: (i) sufficient numbers of immune cells capable of recognizing tumor-associated antigens (TAAs) must be generated *in vivo*; (ii) these cells must distribute to local tumor tissue and infiltrate into the tumor parenchyma; and (iii)

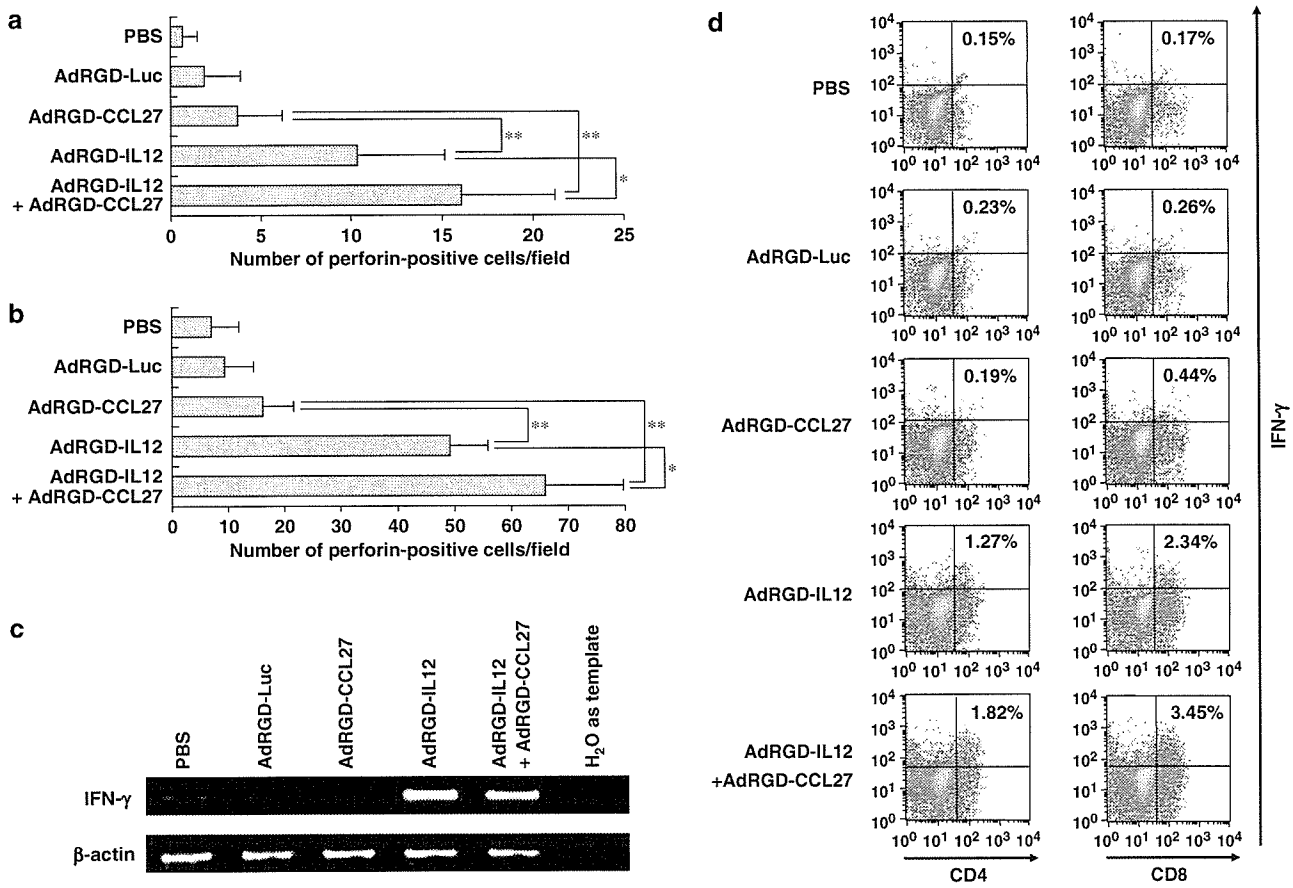

Figure 5 Increases in activated infiltrating lymphocytes in OV-HM and Meth-A tumors injected with the IL-12/CCL27 combination. (**a** and **b**) The number of perforin-positive cells infiltrating into tumor parenchyma was assessed by counting six fields per specimen of immunohistochemical sections against perforin under × 400 magnification. The data represent the mean ± s.d. of results from three tumors. Statistical analysis was carried out using Welch's *t*-test: $^{*}P<0.05$, $^{**}P<0.01$. (**c**) On day 6 after the intratumoral injections, total RNA was isolated from the OV-HM tumors collected from treated mice, and then RT-PCR, specific for IFN-γ and β-actin transcripts, was performed as described in the Materials and methods section. The PCR products were electrophoresed through a 1.5% agarose gel, stained with ethidium bromide and visualized under ultraviolet light. (**d**) On day 6 after the intratumoral injections, single-cell suspensions were prepared by enzymatic digestion of Meth-A tumors as described in the Materials and methods section. Isolated cells were stained with mAbs specific for CD4, CD8 or IFN-γ, and then analyzed by flow cytometer. The percentage value in each panel expresses the percentage of CD4/IFN-γ or CD8/IFN-γ double positive cells.

the tumor-infiltrating immune cells must be activated to manifest appropriate effector mechanisms, such as direct cell lysis and cytokine secretion, capable of causing tumor destruction. It is widely believed that T cells represent the most potent antitumor effector cells and various vaccine strategies including administration of TAA-component vaccines,[26] TAA-coding DNA vaccines,[27] genetically modified tumor cell-based vaccines[28,29] or TAA-delivered DC-based vaccines,[30–32] can both induce and amplify TAA-restricted CTLs and Th cells in patients with cancer. However, excellent therapeutic efficacy, evidenced by marked tumor regression and complete response, has not been reported in a clinical setting to date. One potential cause of these disappointing results is insufficient investigation and understanding of methods that improve accumulation of immune effector cells in tumor tissue, because most conventional studies of cancer immunotherapy have focused on efficient induction and activation of immune effector cells. Even if effector cells exhibiting the ability to kill tumor cells were adequately induced in a patient, the efficacy of cancer immunotherapy would be considerably limited if these effector cells were unable to infiltrate tumor tissue and thereby come in contact with tumor cells. Therefore, innovative approaches capable of better controlling the trafficking and biodistribution of immune effector cells are considered critical for overcoming the limitations of current therapies.

As chemokines regulate leukocytic migration and infiltration of local sites, they are now considered important molecules for augmenting tumor-infiltrating immune cells in cancer immunotherapy. In fact, recent studies in several murine tumor models have provided experimental evidence that introduction of chemokines into the tumor environment results in the recruitment of relevant leukocyte subsets and decreases tumorigenicity of malignant cells.[16–23] However, most of these studies used *ex vivo* gene transfection methods that are not suitable for use within clinical settings, especially for the treatment of patients with established malignancies, and few reports have showed that direct *in vivo* transduction with chemokine genes alone could induce complete

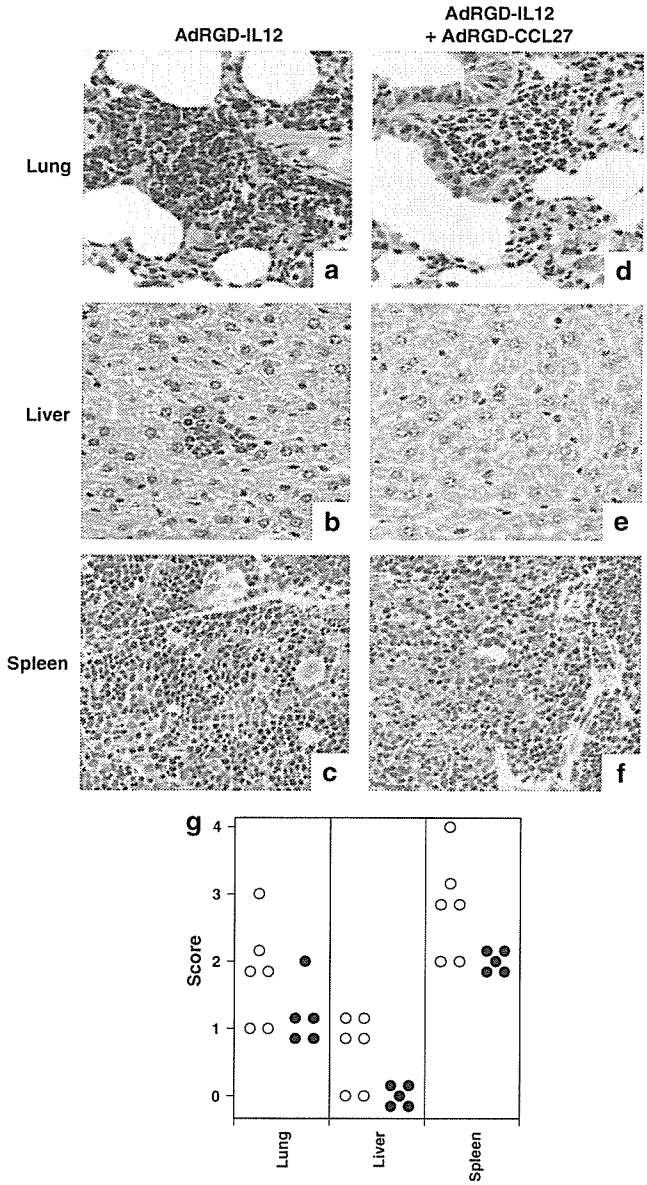

Figure 6 Histopathological examination of lung, liver and spleen in Meth-A tumor-bearing mice treated with the IL-12/CCL27 combination intratumoral injection. BALB/c mice were intradermally inoculated with 2×10^6 Meth-A cells into the flanks. The tumors (7–9 mm in diameter) were injected with AdRGD-IL12 alone or the AdRGD-IL12 and AdRGD-CCL27 combination in a ratio of 9:1 at the same dose totaling 2×10^7 PFU. Three months later, lung (**a** and **d**), liver (**b** and **e**) and spleen (**c** and **f**) were harvested from mice in which the primary tumors were judged to have completely regressed, and then HE staining was performed using paraffin-embedded tissue sections. Original magnifications are $\times 300$. (**g**): Histopathological changes (lymphocyte infiltration in lung and extramedullary hematopoiesis in liver and spleen) were scored as: 0, no; 1, rare; 2, mild; 3, moderate; 4, severe. (○) AdRGD-IL12 alone; (●) AdRGD-IL12 plus AdRGD-CCL27. For extramedullary hematopoiesis in liver and spleen, significant differences ($P < 0.05$) were observed between AdRGD-IL12 plus AdRGD-CCL27 group and AdRGD-IL12 alone group in Mann–Whitney *U*-test.

regression of pre-existing tumor mass. Our previous work also demonstrated that whereas intratumoral injections of AdRGD carrying one chemokine, CCL19, could attract massive numbers of T lymphocytes in established murine B16BL6 melanomas, the antitumor efficacy of this treatment was very modest, resulting in only a slight delay of tumor growth.[23] These results strongly suggested that the augmentation of tumor-infiltrating immune cells due to chemokine gene transduction in itself is insufficient, and that subsequent activation of the recruited immune cells by another treatment is required for the induction of excellent antitumor response. On the other hand, in a number of animal models, multifunctional cytokines, such as IL-2 and IL-12, demonstrate strong antitumor activity by promoting the proliferation and activation of T and NK cells, and by overcoming some immunosuppressive factors in tumor tissues. Although the utility of recombinant protein therapy or gene therapy using these immunomodulators has been widely inspected in clinical trials, a major drawback involves serious adverse effects caused by high systemic peak concentrations associated with large or frequent doses.[11,12] Therefore, establishing a combinational approach, which can maximize the benefits of both chemokines and immunostimulating cytokines, is necessary when designing optimal immunotherapy for malignancies. Dilloo *et al.*[33] reported that *in vitro* cotransfection with the chemokine XCL1 and the cytokine IL-2 into A20 tumor cells using retrovirus vectors greatly expanded tumor-infiltrating T cells attracted by XCL1 and protected against the growth of established tumors in a $CD4^+$ and $CD8^+$ T-cell-dependent manner. Also, Emtage *et al.*[34] demonstrated that intratumoral injection with double-recombinant adenoviral vectors expressing XCL1 along with either IL-2 or IL-12 could elicit potent and long-lasting antitumor responses. These approaches, termed 'attraction-expansion', are based on the assumption that if more immune cells could be recruited to the tumor site by chemokines and subsequently activated by cytokines, the antitumoral immune response could then be significantly enhanced.

In the present study, we selected as a co-stimulator, a chemokine CCL27 – which in our *ex vivo* transfection model[21] could attenuate tumorigenicity of murine OV-HM ovarian carcinoma cells by augmenting tumor-infiltrating T and NK cells – for promoting the antitumor efficacy and improving the safety of IL-12 gene therapy for established tumors. OV-HM tumors are relatively responsive to IL-12-based therapy; in contrast, systemic administration of IL-12 fails to inhibit Meth-A tumor growth because of a lack of immune cell migration and infiltration into tumor stroma.[14,15] In the present therapeutic experiments using AdRGDs capable of efficient gene transduction in various tumors, the IL-12 and CCL27 combinational treatment demonstrated excellent antitumor effects against both established OV-HM and Meth-A tumors compared with treatment with either vector alone, and, more importantly, induced complete tumor regression in all tested OV-HM tumor-bearing mice and in 12 of 13 Meth-A tumor-bearing mice. Moreover, the antitumor responses elicited by the combinational therapy with AdRGD-IL12 and AdRGD-CCL27 were tumor-specific and long lasting as determined by rechallenge experiments and hence demonstrated a protective immunity. These data indicate that synergic effects arising from the IL-12/CCL27 combination may promote more efficacious and safer IL-12 gene therapy for cancer at doses lower than the maximum tolerance dosage.

Therefore, we also investigated the antitumoral mechanisms associated with the synergy of IL-12 and CCL27 by *in vivo* depletion assays and immunohistochemical analysis. The immune system is roughly classified into cellular immunity and humoral immunity, and an optimal immune response is achieved by the balanced activation of both systems. Cellular immune responses including the activation of NK cells and CTLs play a more important role in elimination of tumor cells by tumor immunity than humoral immune responses accompanied by antibody production from B cells. The antitumor effects in the IL-12/CCL27 combinational therapy were T-cell-dependent, with the effector activity of $CD8^+$ CTLs, rather than with the NK activity, mainly contributing to the regression of the pre-existing tumors. This finding reasonably accounts for the generation of systemic long-term specific immunity in mice receiving the IL-12/CCL27 combinational therapy because T-cell-dependent immunity possesses both effector and memory phases. In addition, tumors injected with the IL-12/CCL27 combination showed more enhanced accumulation of $CD3^+$ T cells than those injected with AdRGD-IL12 alone, whereas treatment with AdRGD-CCL27 alone was the most effective. This result demonstrates that CCL27 is a strong recruiter for T cells into tumor tissue, and is consistent with our previous data in an *ex vivo* transfection model.[21] In T-cell subset analysis, the IL-12/CCL27-treated group induced the infiltration of $CD8^+$ CTLs – the major effector cells in the *in vivo* depletion assays – into tumor parenchyma more efficiently than the group treated with AdRGD-CCL27 alone even though the total vector dosage of AdRGD-CCL27 in the former was only one-tenth of that in the latter. Moreover, the infiltrating immune cells in tumors treated with AdRGD-IL12 alone or IL-12/CCL27 together were highly activated, as determined by the number of perforin-positive cells and IFN-γ-producing T cells in tumor tissue. On the other hand, most of the immune cells recruited by injection with AdRGD-CCL27 alone were in an inactivated or naive state, explaining why treatment with AdRGD-CCL27 alone did not show significant antitumor effects in spite of its ability to augment T-cell-infiltration. IL-12 can activate signal transducer and activator of transcription (STAT)4 via binding to its receptor, and STAT4 plays an important role within the microenvironment for Th1-biased immune responses, by expressing a set of genes such as IFN-γ and IL-18 receptor α subunit.[35] In addition, the cellular immune response including effector activity of CTLs and NK cells is dominantly activated by the helper function of Th1 cells.[36] On the basis of our current results, we determined that the synergic antitumor responses in the IL-12/CCL27 combinational therapy reflected both the CCL27-induced augmentation of tumor-infiltrating immune cells and the subsequent IL-12-stimulated enhancement of effector activity.

In our experimental models, mice achieving complete regression of the primary tumors because of AdRGD-IL12 treatment alone showed some histopathological changes within lung, liver and spleen, for example lymphocyte infiltration and extramedullary hematopoiesis. Although the mechanisms associated with these peripheral adverse effects remain unclear, we speculate that IL-12 spreading into the systemic blood circulation from tumor tissues potentiated peripheral hematopoiesis because the administration of recombinant IL-12 results in significant splenic hyperplasia with increased progenitor cells, increased circulating progenitor cells and bone marrow hypoplasia with decreased progenitor cells in a time- and dose-dependent manner.[37,38] On the other hand, the IL-12/CCL27 combinational treatment could reduce the side effects observed after complete tumor regression, suggesting that most of the IL-12 produced in tumor tissues might have been utilized for local activation of tumor-infiltrating immune cells; this improved therapeutic safety was probably related to the consumption of intratumoral IL-12 by recruited immune cells.

In conclusion, our results revealed that cotransduction with IL-12 and CCL27 genes into established tumors by using AdRGD could promote antitumor responses through both the recruitment and activation of tumor-infiltrating immune cells, and would greatly contribute to the development of an efficacious and safe cancer immunogene therapy. At present, in order to expand our combinational cancer immunogene therapy to metastatic tumors, in which intratumoral injection of vectors is physically difficult, we are pushing forward with the development of vectors, which can be transductionally and transcriptionally targeted to tumors and also with methods to specifically deliver therapeutic genes into tumor cells by systemic administration.[39–41]

Materials and methods

Cell lines and mice

Murine ovarian carcinoma OV-HM cells ($H\text{-}2^{b/k}$) and murine fibrosarcoma Meth-A cells ($H\text{-}2^{d}$) were kindly provided by Dr Hiromi Fujiwara. Murine colon adenocarcinoma CT26 cells ($H\text{-}2^{d}$) were kindly provided by Professor Nicholas P Restifo (National Cancer Institute, Bethesda, MD, USA). OV-HM and CT26 cells were grown in RPMI 1640 supplemented with 10% fetal bovine serum (FBS). Meth-A cells were maintained by intraperitoneal passage in syngeneic BALB/c mice. HEK293 cells, the helper cell line for AdRGD-propagation, were purchased from ATCC (Manassas, VA, USA). B16BL6 cells ($H\text{-}2^{b}$), a melanoma cell line originating from C57BL/6 mice, were distributed from the Cell Resource Center for Biomedical Research, Institute of Development, Aging and Cancer, Tohoku University (Sendai, Japan). HEK293 cells and B16BL6 cells were cultured in Dulbecco's modified Eagle's medium supplemented with 10% FBS. Female (C57BL/6 × C3H/He) F1 (B6C3F1) mice, BALB/c mice and BALB/c nude mice were purchased from Japan SLC Inc. (Hamamatsu, Japan), and were used at 6–8 weeks of age. Animal experimental procedures were in accordance with the Osaka University guidelines for the welfare of animals in experimental neoplasia.

Vectors

Because most malignant tumors express little coxsackie-adenovirus receptor, which is the primary receptor for conventional adenoviral vectors, we utilized AdRGDs, which are infectivity-enhanced adenoviral vectors with an RGD-4C motif in the adenoviral fiber-knob region. Replication-deficient AdRGD was based on the adenovirus serotype 5 backbone with deletions of E1 and E3 regions. The RGD-4C sequence for αv-integrin-targeting was inserted into the HI loop of the fiber knob using a two-step method, as previously described.[42] AdRGD-

IL12,[13] AdRGD-CCL27,[21] and AdRGD-Luc[42] under the control of the cytomegalovirus promoter were previously constructed by an improved *in vitro* ligation method.[42–44] All recombinant AdRGDs were propagated in HEK293 cells, purified by two rounds of cesium chloride gradient ultracentrifugation, dialyzed, and stored at −80°C. Titers of infective AdRGD particles (PFU) were evaluated by the end-point dilution method using HEK293 cells.

Tumor inoculation and intratumoral administration of vectors in animal experiments

B6C3F1 mice, BALB/c mice or BALB/c nude mice were intradermally inoculated with 10^6 OV-HM cells or 2×10^6 Meth-A cells into the flank. After established tumor diameters reached 7–9 mm, AdRGD-IL12 alone, AdRGD-CCL27 alone or AdRGD-IL12 plus AdRGD-CCL27 in a ratio of 1:9, 1:1 or 9:1 were intratumorally injected at a total of 2×10^7 PFU in 50 μl PBS. AdRGD-Luc was used as a control vector. Tumor growth was monitored twice or three times a week by measurement of the major axis of the tumors using microcalipers. The data were expressed as a relative tumor size to the initial tumor size. The mice were euthanized when the tumor measurements were greater than 20 mm. On day 90 after treatment, mice without palpable tumor masses were judged to be individuals that could potentially achieve complete regression.

Tumor rechallenge experiments in mice achieving complete regression of primary tumors

Three or six months after treatment with the combination of AdRGD-IL12 and AdRGD-CCL27 in a 9:1 ratio totaling 2×10^7 PFU, mice that achieved complete regression of primary tumors were rechallenged with 10^6 OV-HM cells, 3×10^5 B16BL6 cells, 10^6 Meth-A cells or 3×10^5 CT26 cells by intradermal injection into the opposite flank of the first tumor inoculation. On day 60 after tumor rechallenge, the tumor-free mice were judged to be individuals that had achieved complete tumor rejection.

In vivo *depletion analysis*

Ascites from BALB/c nude mice intraperitoneally injected with GK1.5 hybridoma (anti-CD4)[45] or 53–6.72 hybridoma (anti-CD8)[46] were kindly provided by Professor Hiroshi Yamamoto (Department of Immunology, Graduate School of Pharmaceutical Sciences, Osaka University, Osaka, Japan). Mice bearing OV-HM or Meth-A tumor were intratumorally injected with the combination of AdRGD-IL12 and AdRGD-CCL27 in a ratio of 9:1 totaling 2×10^7 PFU on day 0, and intraperitoneally injected seven times on days −3, −2, −1, 0, 5, 10 and 15 with 100-μl GK1.5 or 53–6.72 ascites, or 40-μl rabbit anti-asialoGM1 antiserum (Wako Pure Chemical Industries, Ltd, Osaka, Japan). The depletion of T-cell subsets and NK cells was confirmed by flow cytometric analysis of peripheral blood and splenic cells. Tumor growth was monitored as described above. The mice were euthanized when the tumor measurements were greater than 20 mm.

Immunohistochemical examination of tumor sections

Tumor-bearing mice were killed 6 days after the intratumoral injection of AdRGD. For immunohistochemical analysis, the fresh tumor nodules were embedded in OCT compound (Sakura Finetechnical Co., Ltd, Tokyo, Japan), and frozen in liquid nitrogen. Frozen sections (6 μm in thickness) were fixed in 4% paraformaldehyde, washed with PBS and then stored at −80°C until needed for subsequent procedures. The immunostaining procedures, which included blocking for endogenous peroxidase activity with peroxidase blocking solution (Dako Japan Co., Ltd, Kyoto, Japan), blocking for nonspecific binding of the subsequently used immunoreagents with 5% bovine serum albumin, incubation with optimal dilution of antibody, incubation of reagent(s) for detection, and development with 3,3′-diaminobenzidine, were carried out on an automated immunostaining system (Autostainer Plus, Dako Japan). Between all incubation steps, the tumor sections were washed with Tris-buffered saline containing Tween-20. The following were used as primary antibodies: rabbit anti-human CD3 polyclonal antibody (Dako Japan), rat anti-mouse CD4 monoclonal antibody (mAb) (RM4-5; BD Biosciences, San Jose, CA, USA), rat anti-mouse CD8 mAb (KT15; Serotec Co., Ltd, Sapporo, Japan) and rat anti-mouse perforin mAb (CB5.4; Abcam, Paris, France). Rabbit anti-human CD3 polyclonal antibody was detected with ENVISION+ Rabbit/HRP (Dako Japan). Other primary antibodies were detected with HRP-conjugated anti-rat Ig (Santa Cruz Biotechnology, Inc., Santa Cruz, CA, USA) and CSA II System (Dako Japan). The sections were finally counterstained with hematoxylin. The numbers of immunostained cells in six fields per specimen were counted under a light microscope using × 400-magnification.

RT-PCR analysis for IFN-γ expression levels in tumor tissues

OV-HM tumors were collected 6 days after intratumoral injection of AdRGD, and total RNA was isolated using TRI Reagent (SIGMA-ALDRICH Japan, Tokyo, Japan) according to the manufacturer's instructions. RT proceeded for 60 min at 50°C in a 20 μl reaction mixture containing 2 μg total RNA treated with DNase I, 4 μl 5 × RT buffer, 0.1 M dithiothreitol, 0.1 mM dNTP mix, 0.5 μg oligo $(dT)_{20}$, 1 μl RNase inhibitor and 1 μl SuperScript III (Invitrogen, Carlsbad, CA, USA). PCR amplification of IFN-γ and β-actin transcripts was performed in a 50 μl reaction mixture containing 2 μl of RT-material, 5 μl 10 × PCR buffer, 0.25 μl Ampli *Taq* DNA polymerase (TOYOBO Co., Ltd, Osaka Japan), 1 μl dimetylsulfoxide, 0.2 mM dNTP and 0.4 μM primers. The sequences of the specific primers were as follows; murine IFN-γ: forward, 5′-gct ttg cag ctc ttc ctc at-3′; reverse, 5′-tga gct cat tga atg ctt gg-3′; murine β-actin: forward, 5′-tgt gat ggt ggg aat ggg tca g-3′; reverse, 5′-ttt gat gtc acg cac gat ttc c-3′. After denaturation for 4 min at 96°C, 3 sequential steps, denaturation for 30 s at 96°C, annealing for 30 s at 60°C and extension for 30 s at 72°C, were repeated for 30 cycles, ending with a final extension step for 4 min at 72°C. The PCR products was electrophoresed through a 1.5% agarose gel, stained with ethidium bromide and visualized under ultraviolet radiation. The expected PCR product sizes were 379 bp (IFN-γ) and 514 bp (β-actin).

Flow cytometric analysis for tumor-infiltrating T cells

Meth-A tumors were dissected 6 days after intratumoral injection of AdRGD, and then chopped into small pieces

using a razor blade before incubation with a mixture of collagenase (1 mg/ml, Wako Pure Chemical Industries, Ltd) dissolved in Hanks' balanced salt solution for 60 min at 37°C. The cells were passed through a 70-μm nylon strainer to remove any debris, recovered by centrifugation and resuspended in complete medium. Then, the cell suspension was overlaid on 40 and 80% Percoll gradient and centrifuged at 2000 r.p.m. for 20 min at room temperature. After centrifugation, cells deposited at the interface were harvested and washed two times with complete medium. Phenotype of T cells isolated from tumors treated with various AdRGD was confirmed by flow cytometric analysis. Briefly, 10^6 cells were incubated on ice for 20 min with 100 μl of staining buffer (PBS containing 2% FBS and 0.09% NaN_3) containing anti-FcγRII/III mAb (93, rat $IgG_{2a,\lambda}$; eBioscience, San Diego, CA, USA) to block nonspecific binding of the subsequently used mAbs, and then the cells were stained with FITC-conjugated anti-mouse CD4 mAb (GK1.5, rat $IgG_{2b,\kappa}$; eBioscience) or FITC-conjugated anti-mouse CD8 mAb (53–6.7, rat $IgG_{2a,\kappa}$; eBioscience). After incubation for 20 min, cells were washed with staining buffer, fixed with Cytofix/Cytoperm Buffer (BD Biosciences) for 15 min and permeabilized with Perm/Wash Buffer (BD Biosciences). Intracellular IFN-γ was stained with PE-conjugated anti-mouse IFN-γ mAb (XMG1.2, rat $IgG_{1,\kappa}$; BD Biosciences). After incubation for 20 min, the stained cells were analyzed for CD4/CD8 and IFN-γ expression by a FACSCalibur flow cytometer using CellQuest software (BD Biosciences).

Histopathological examination of tissue sections

Tumor-regressed mice were killed 3 months after the intratumoral injection with AdRGD-IL12 alone or the combination of AdRGD-IL12 and AdRGD-CCL27 in a ratio of 9:1 totaling 2×10^7 PFU. The lungs, liver and spleen were harvested from each of these mice, placed in neutral 10% formalin/PBS and embedded in paraffin. Sections (5 μm) were prepared for hematoxylin and eosin (HE) staining, and then histopathological examination was performed at Applied Medical Research Laboratory (Osaka, Japan).

Abbreviations

AdRGD, RGD fiber-mutant adenoviral vector; CCL, CC-chemokine ligand; CTL, cytotoxic T lymphocyte; DC, dendritic cell; FBS, fetal bovine serum; HE, hematoxylin and eosin; IFN, interferon; IL, interleukin; mAb, monoclonal antibody; NK, natural killer; PBS, phosphate-buffered saline; PFU, plaque-forming unit; RT-PCR, reverse transcription-polymerase chain reaction; STAT, signal transducer and activator of transcription; TAA, tumor-associated antigen; Th, helper T

Acknowledgements

We are grateful to Professor Osamu Yoshie and Dr Takashi Nakayama (Department of Microbiology, Kinki University School of Medicine, Osaka-Sayama, Japan) for providing a plasmid-containing murine CCL27 cDNA, to Professor Hiroshi Yamamoto (Department of Immunology, Graduate School of Pharmaceutical Sciences, Osaka University, Osaka, Japan) for providing murine IL-12 cDNA-containing plasmid, GK1.5 ascites and 53–6.72 ascites, to Dr Hiromi Fujiwara for providing OV-HM and Meth-A cells, to Professor Nicholas P Restifo (National Cancer Institute, Bethesda, MD, USA) for providing CT26 cells and to Mr Alexandre Learth Soares and Mr Feng Qiu (Department of Biotechnology and Therapeutics, Graduate School of Pharmaceutical Sciences, Osaka University, Osaka, Japan) for their technical assistance. The present study was supported in part by grants from the Ministry of Health, Labour and Welfare of Japan, by a Grant-in-Aid for Scientific Research on Priority Areas (17016043) and Young Scientists (A) (18689007) from the Ministry of Education, Culture, Sports, Science and Technology of Japan and by grant from the Takeda Science Foundation.

References

1 Gubler U, Chua AO, Schoenhaut DS, Dwyer CM, McComas W, Motyka R *et al.* Coexpression of two distinct genes is required to generate secreted bioactive cytotoxic lymphocyte maturation factor. *Proc Natl Acad Sci USA* 1991; **88**: 4143–4147.
2 Wolf SF, Temple PA, Kobayashi M, Young D, Dicig M, Lowe L *et al.* Cloning of cDNA for natural killer cell stimulatory factor, a heterodimeric cytokine with multiple biologic effects on T and natural killer cells. *J Immunol* 1991; **146**: 3074–3081.
3 Robertson MJ, Soiffer RJ, Wolf SF, Manley TJ, Donahue C, Young D *et al.* Response of human natural killer (NK) cells to NK cell stimulatory factor (NKSF): cytolytic activity and proliferation of NK cells are differentially regulated by NKSF. *J Exp Med* 1992; **175**: 779–788.
4 Brunda MJ. Interleukin-12. *J Leukoc Biol* 1994; **55**: 280–288.
5 Chan SH, Perussia B, Gupta JW, Kobayashi M, Pospisil M, Young HA *et al.* Induction of interferon-γ production by natural killer cell stimulatory factor: characterization of the responder cells and synergy with other inducers. *J Exp Med* 1991; **173**: 869–879.
6 Chan SH, Kobayashi M, Santoli D, Perussia B, Trinchieri G. Mechanisms of IFN-γ induction by natural killer cell stimulatory factor (NKSF/IL-12). Role of transcription and mRNA stability in the synergistic interaction between NKSF and IL-2. *J Immunol* 1992; **148**: 92–98.
7 Hsieh CS, Macatonia SE, Tripp CS, Wolf SF, O'Garra A, Murphy KM. Development of TH1 $CD4^+$ T cells through IL-12 produced by *Listeria*-induced macrophages. *Science* 1993; **260**: 547–549.
8 Seder RA, Gazzinelli R, Sher A, Paul WE. Interleukin 12 acts directly on $CD4^+$ T cells to enhance priming for interferon γ production and diminishes interleukin 4 inhibition of such priming. *Proc Natl Acad Sci USA* 1993; **90**: 10188–10192.
9 Nastala CL, Edington HD, McKinney TG, Tahara H, Nalesnik MA, Brunda MJ *et al.* Recombinant IL-12 administration induces tumor regression in association with IFN-γ production. *J Immunol* 1994; **153**: 1697–1706.
10 Voest EE, Kenyon BM, O'Reilly MS, Truitt G, D'Amato RJ, Folkman J. Inhibition of angiogenesis *in vivo* by interleukin 12. *J Natl Cancer Inst* 1995; **87**: 581–586.
11 Leonard JP, Sherman ML, Fisher GL, Buchanan LJ, Larsen G, Atkins MB *et al.* Effects of single-dose interleukin-12 exposure on interleukin-12-associated toxicity and interferon-γ production. *Blood* 1997; **90**: 2541–2548.
12 Atkins MB, Robertson MJ, Gordon M, Lotze MT, DeCoste M, DuBois JS *et al.* Phase I evaluation of intravenous recombinant human interleukin 12 in patients with advanced malignancies. *Clin Cancer Res* 1997; **3**: 409–417.